Climate changes:
Assessment of natural and anthropogenic factors and cause-and-effect relations

Igor I. Mokhov

A.M. Obukhov Institute of Atmospheric Physics RAS

mokhov@ifaran.ru

ENVIROMIS-2010

5 July 2010

Zvenigorod Scientific Station of the IAP RAS (55.7°N)

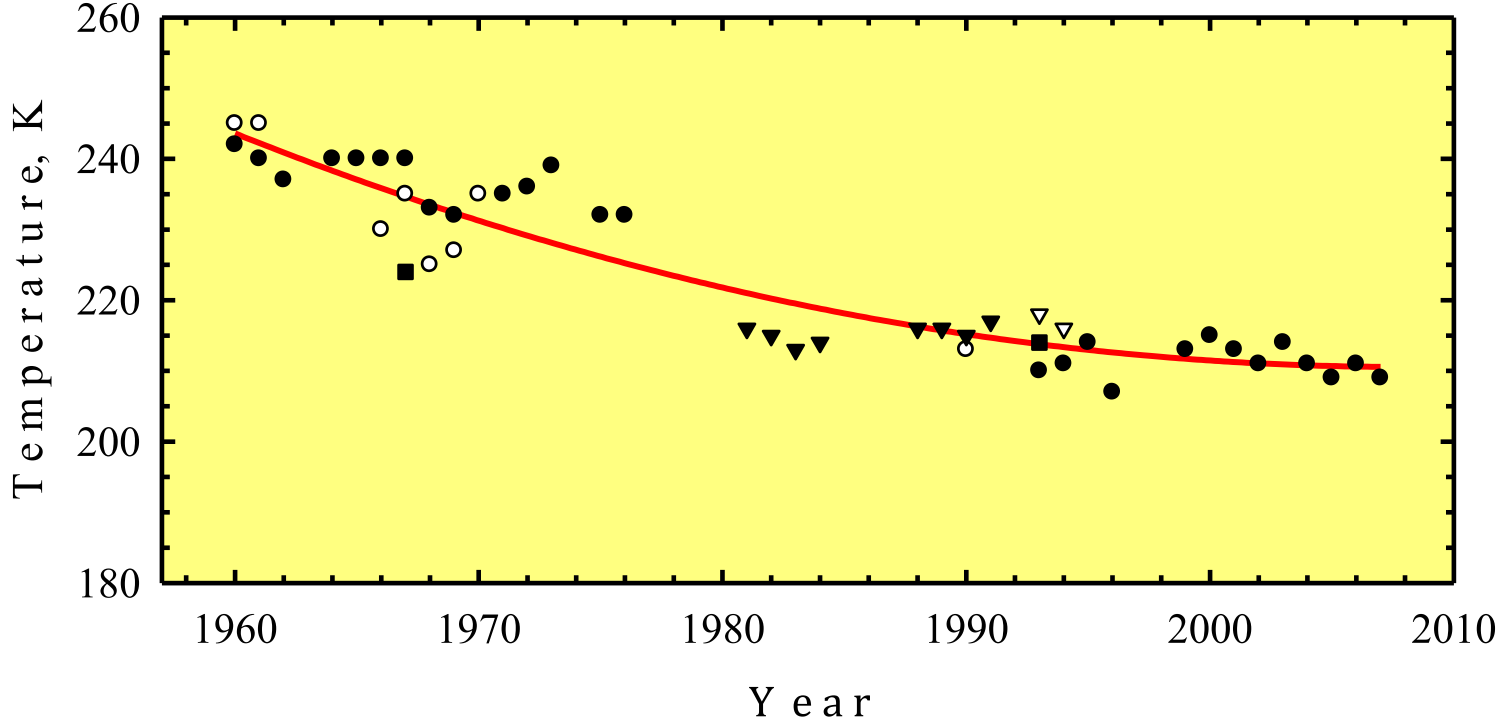

Temperature changes at the mesopause from spectrophotometric measurements of the hydroxyl emission at the Zvenigorod station (full circles with red line as an approximation) in comparison with observations at different middle-latitude stations: Abastumani (41.8°N) - hollow circles, Quebec (46.8°N) and Delaware (42.8°N) - squares, are Wuppertal (51°N) - full inverted triangles, Maynooth (53.2°N) - hollow inverted triangles.

Semenov et al.

Zonal-mean atmospheric temperature changes (K) from 1890 to 1999 from model simulations (PCM) with different forcings: a) solar, b) volcanoes, greenhouse gases, d) ozone changes, e) sulfate aerosol, f) sum of all forcings.

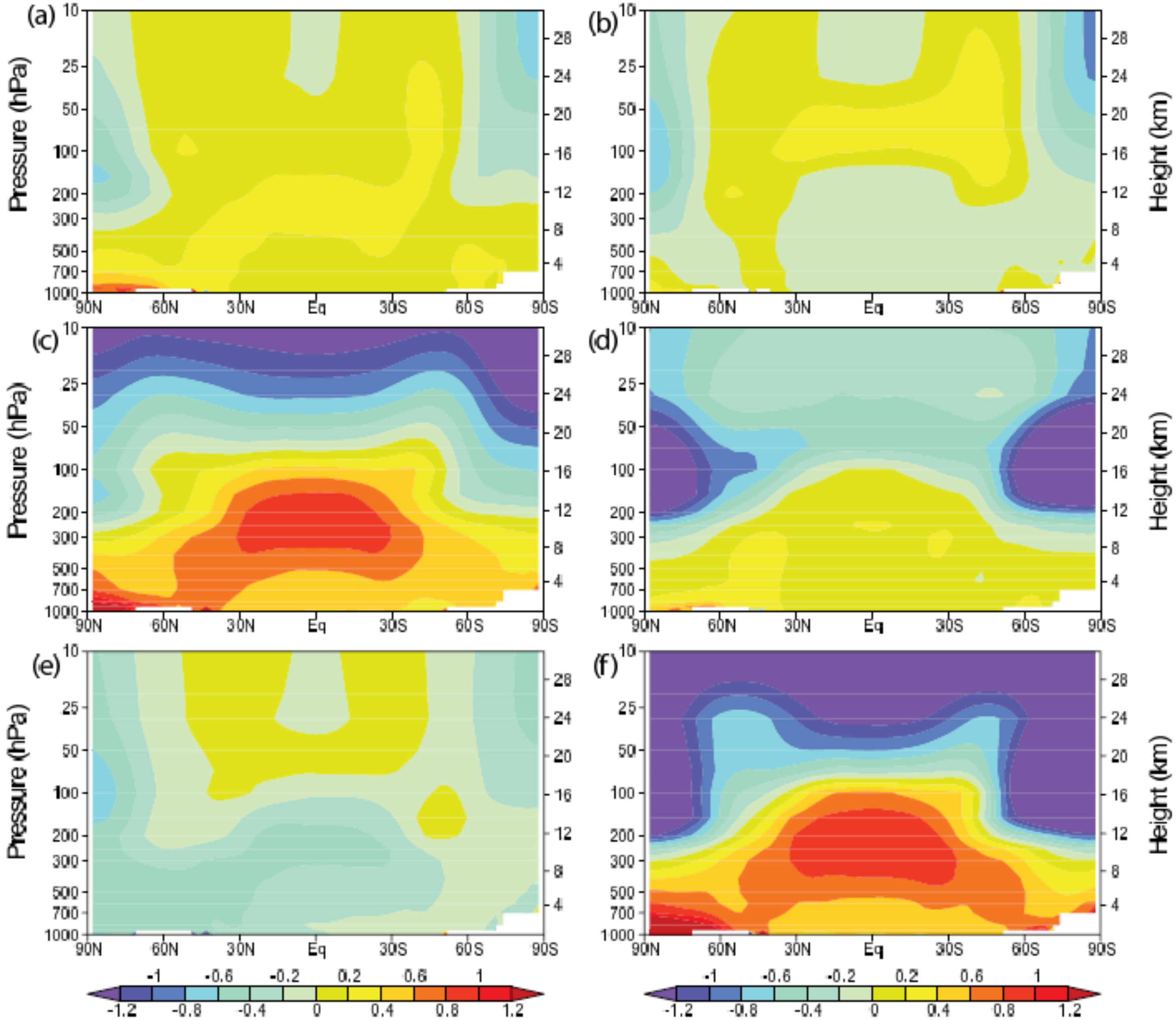

IPCC-2007

Surface temperature changes

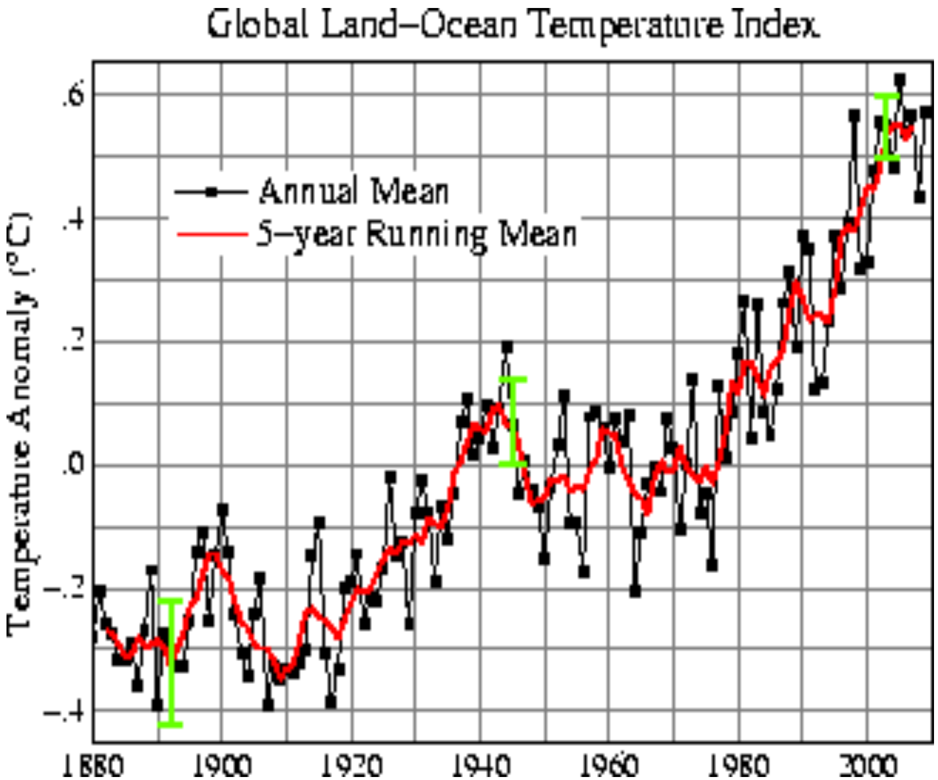

by GISS data

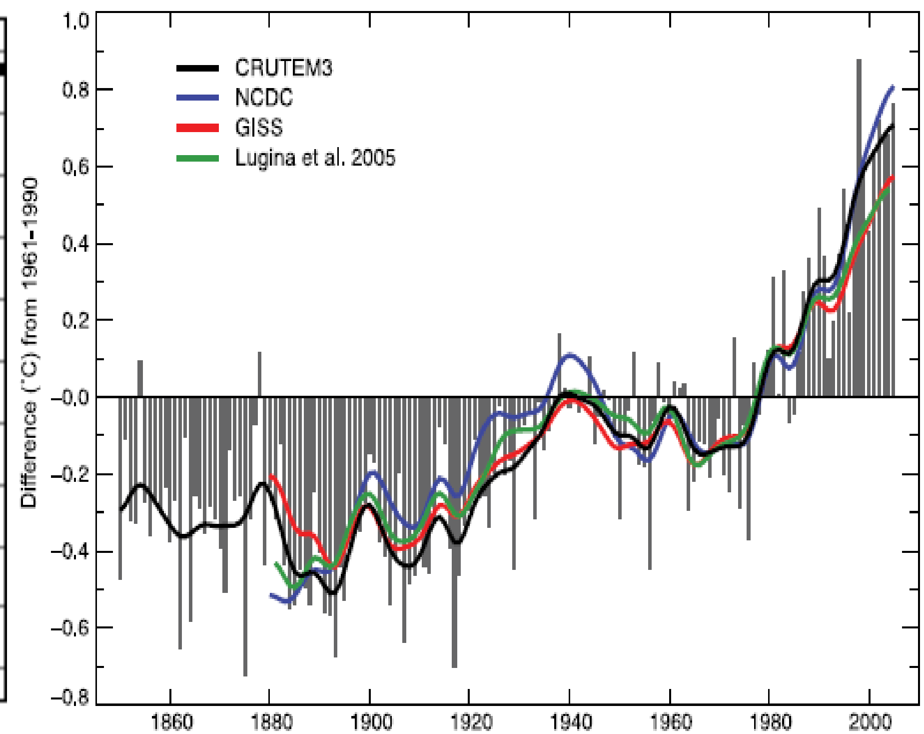

Annual anomalies of global land-surface air temperature (relative to 1961-1990) from different datasets. Smooth curves show decadal variations.

Surface temperature anomalies (K) in January 2006 and January 2010 (relative to 1951-1980)

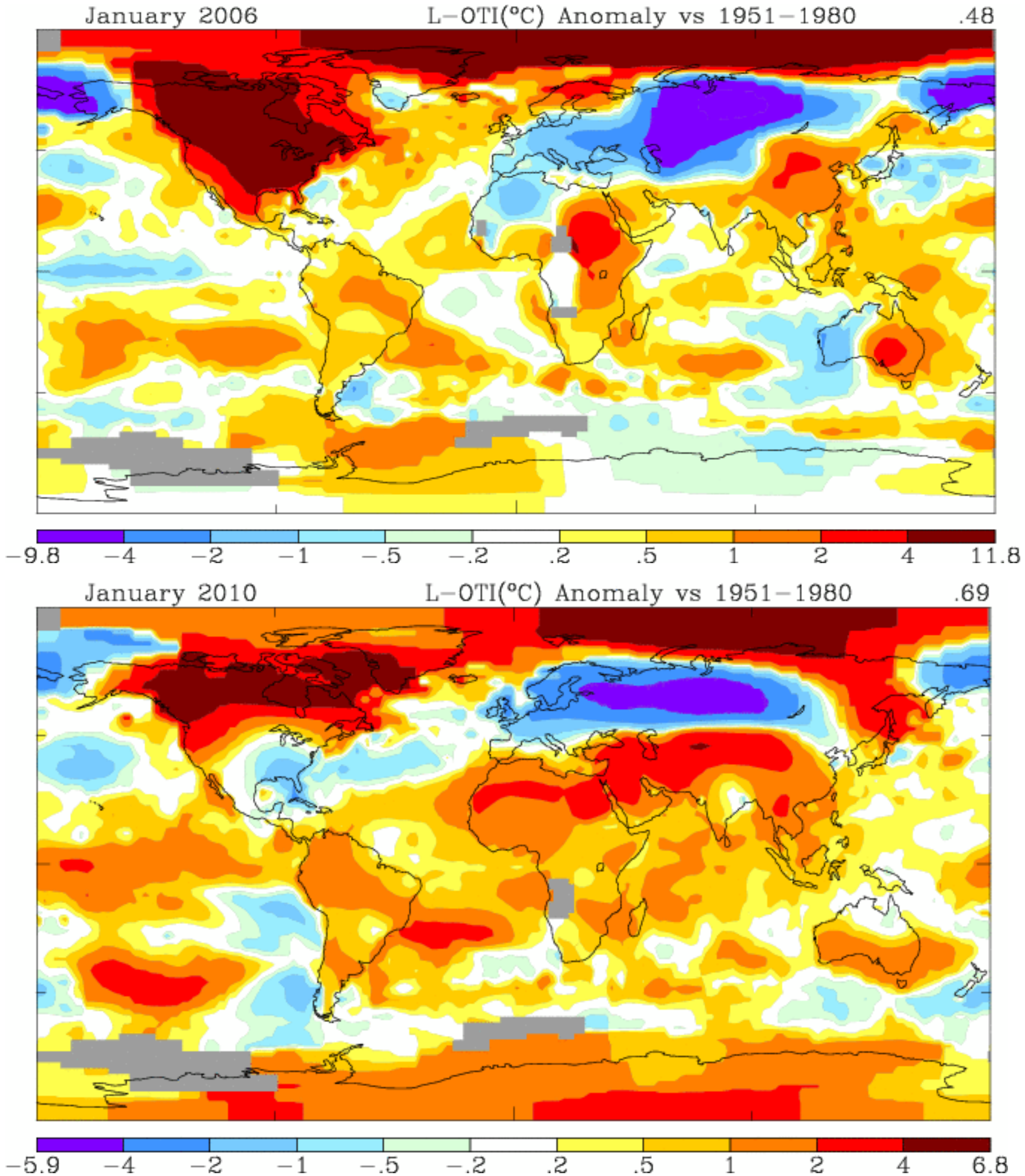

by GISS data

Surface temperature anomalies (K) in Winter 2009-2010 (relative to 1951-1980)

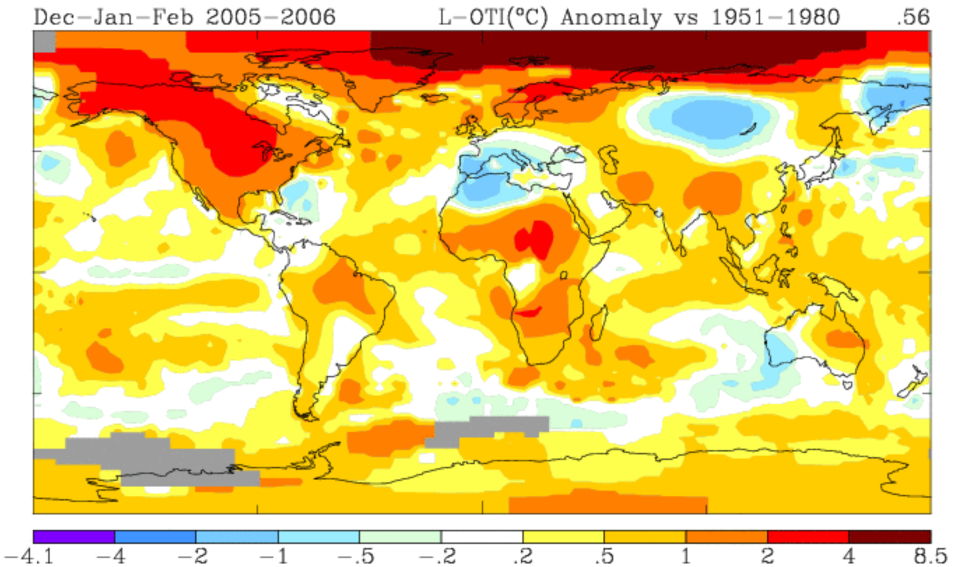

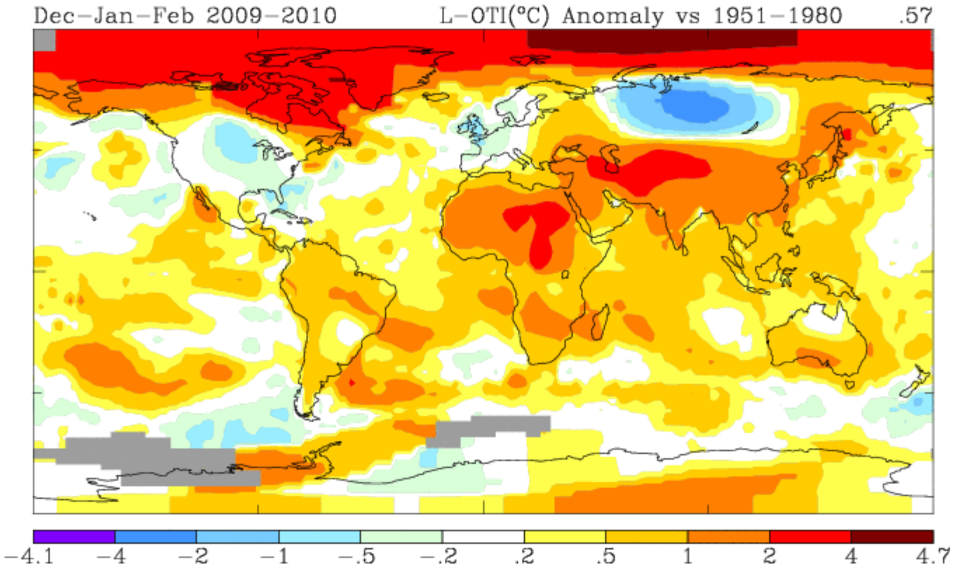

by GISS data

Ratio of the NH blockings action estimates [*energy* x *time*] for 2xCO_2 and 1xCO_2 regimes from model simulations for different seasons and sectors

	VII-IX Summer	X-XII Autumn	I-III Winter	IV-VI Spring	I-XII Annual
Atlantic sector (80°W-40°E)	0.2	1.1	1.2	1.1	1.0
Pacific sector (140°E-100°W)	1.0	0.8	1.0	0.9	0.9
Continents (40-140°E, 100-80°W)	0.8	0.3	4.1	4.6	1.8
Northern Hemisphere	0.7	0.8	1.3	1.4	1.1

Mokhov

Interannual variations of blockings number in the Northern Hemisphere

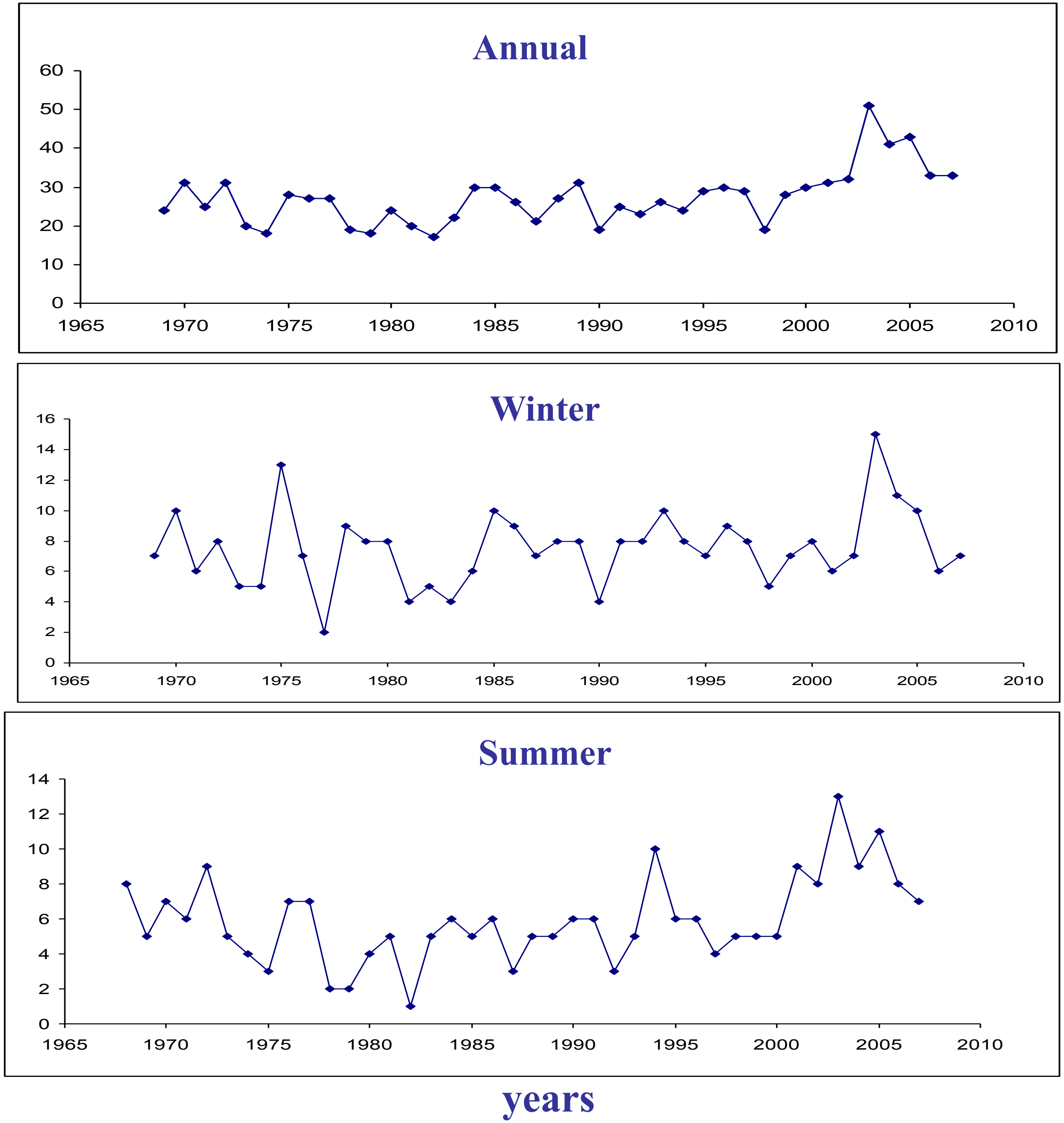

Interannual variations of blockings intensity in the Northern Hemisphere

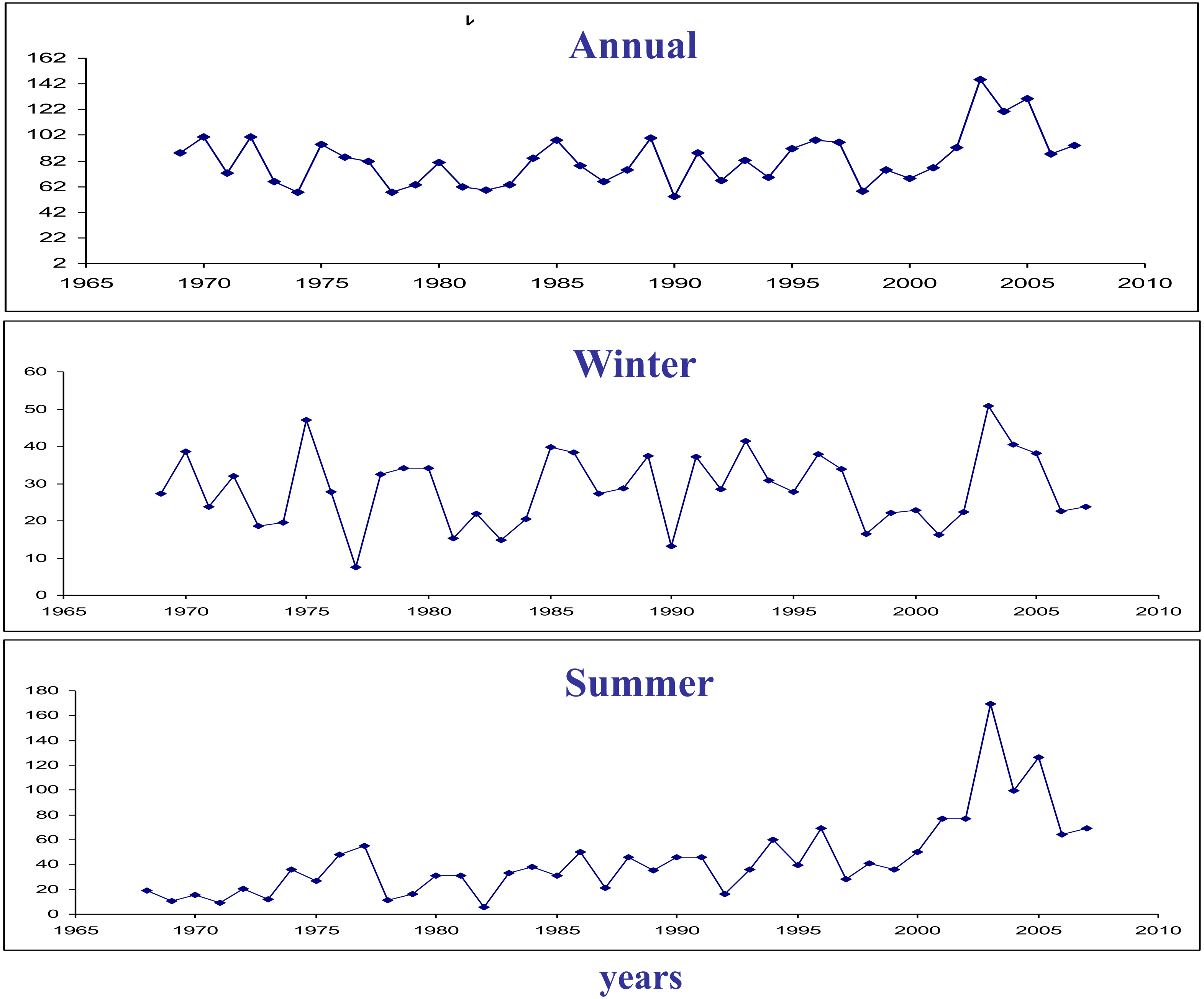

Surface temperature anomalies (K) in 2010 (relative to 1951-1980): a) January, b) February, c) March, d) April

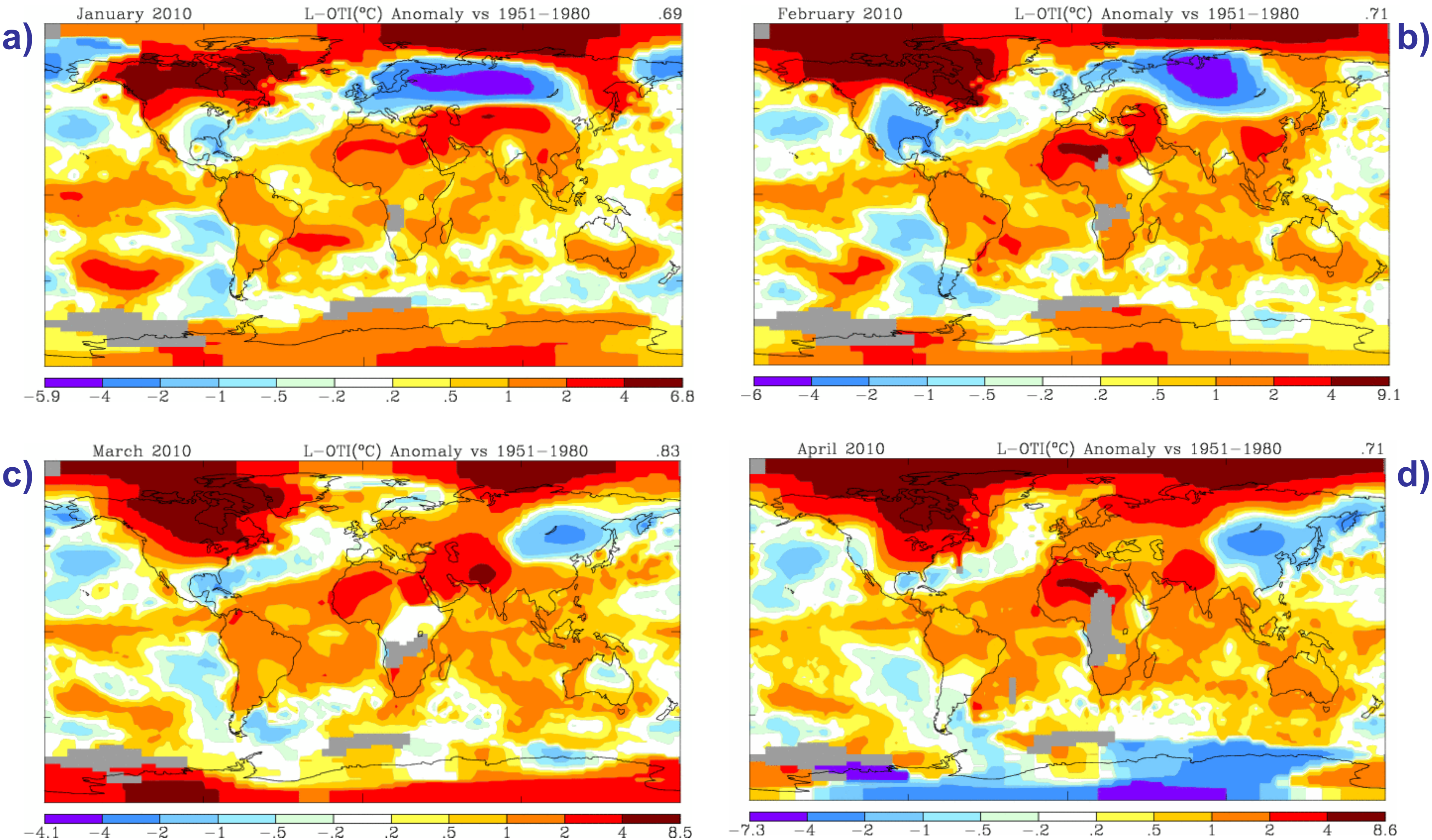

by GISS data

Surface annual-mean temperature anomalies (K) during last decade (2000-2009) (relative to 1951-1980)

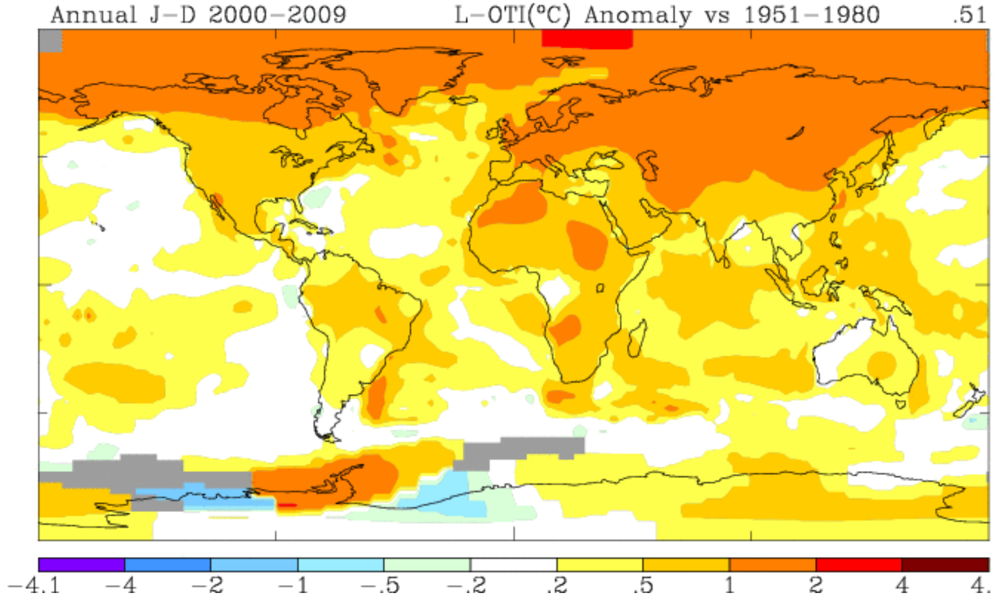

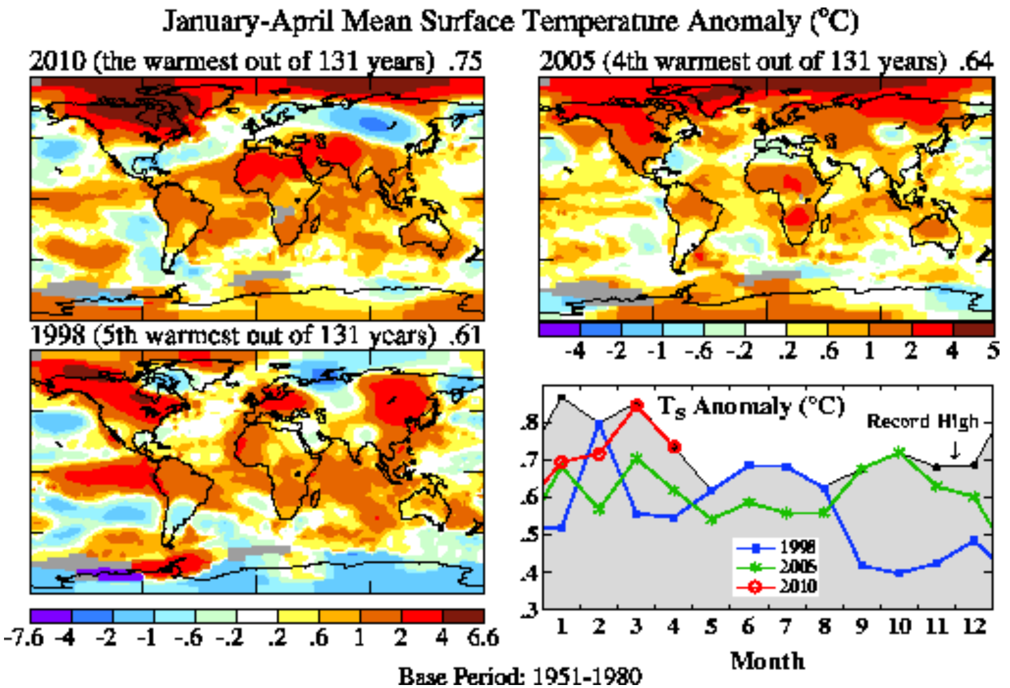

by GISS data

Surface annual-mean temperature changes (K) between 1990s and 1980s

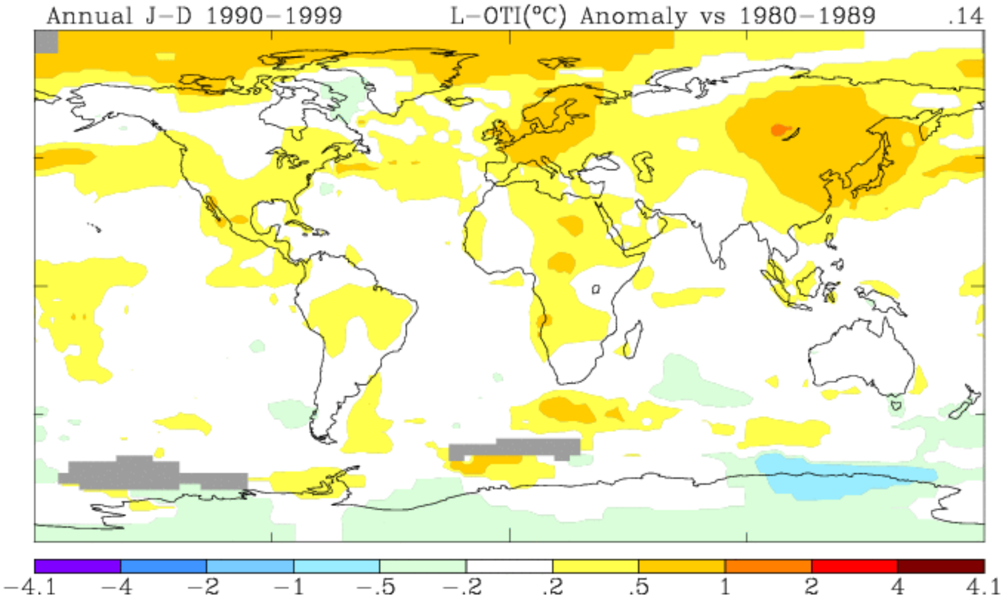

Surface annual-mean temperature changes (K) between 2000s and 1990s

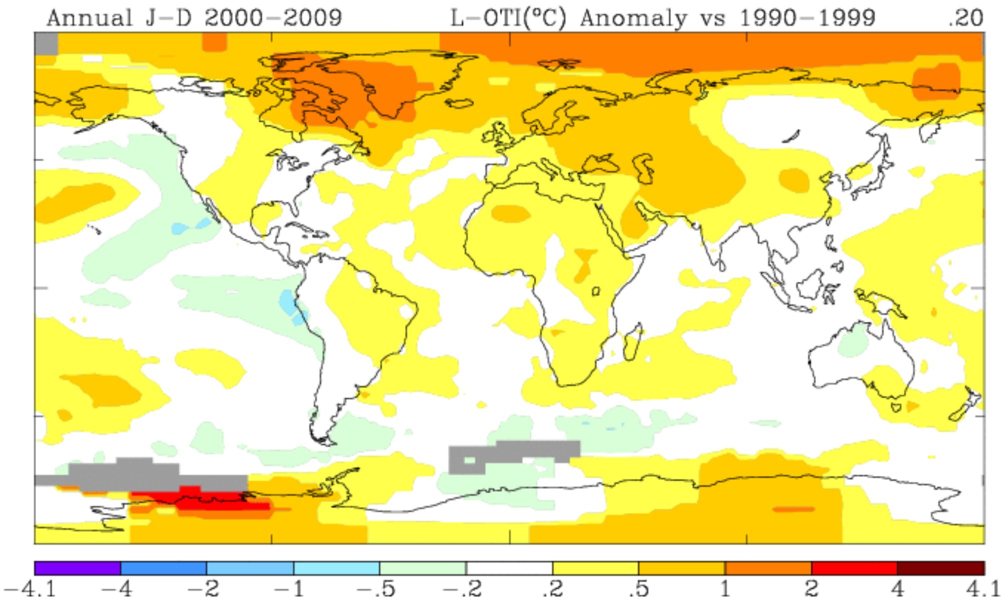

by GISS data

Zonal-mean changes of annul-mean surface temperature by GISS data

(1990-1999)-(1980-1989)

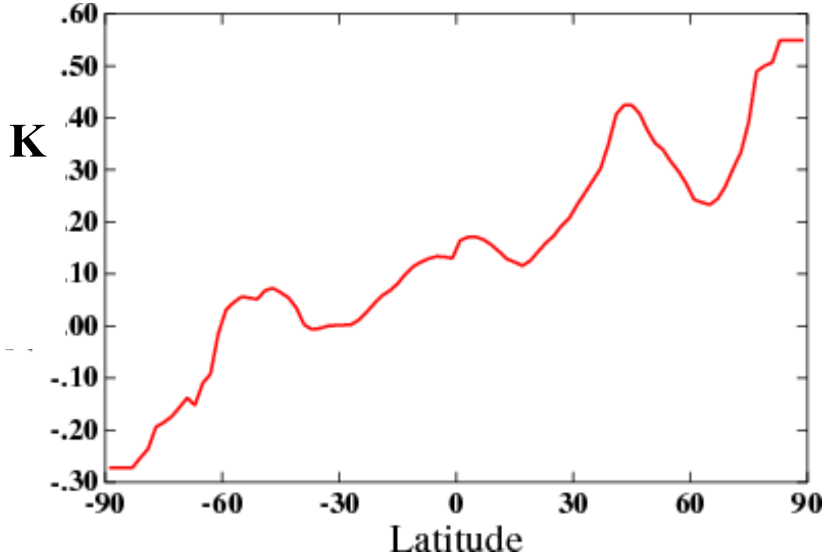

(2000-2009)-(1990-1999)

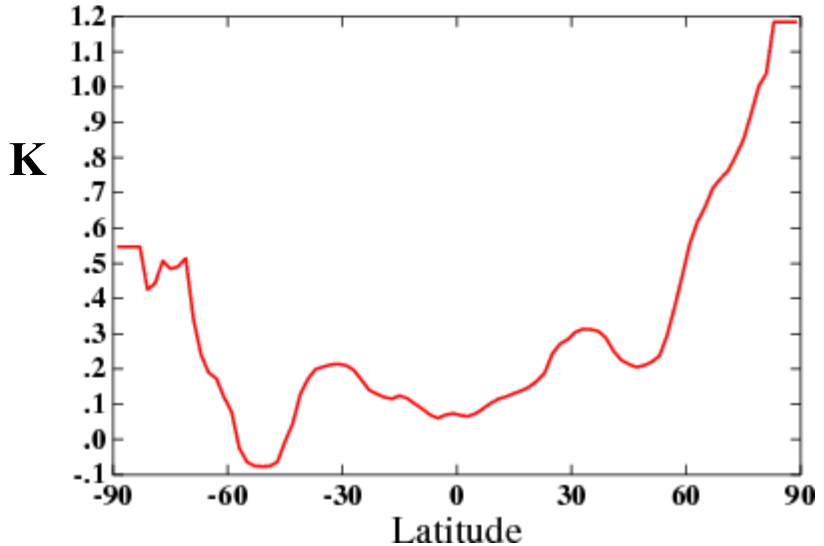

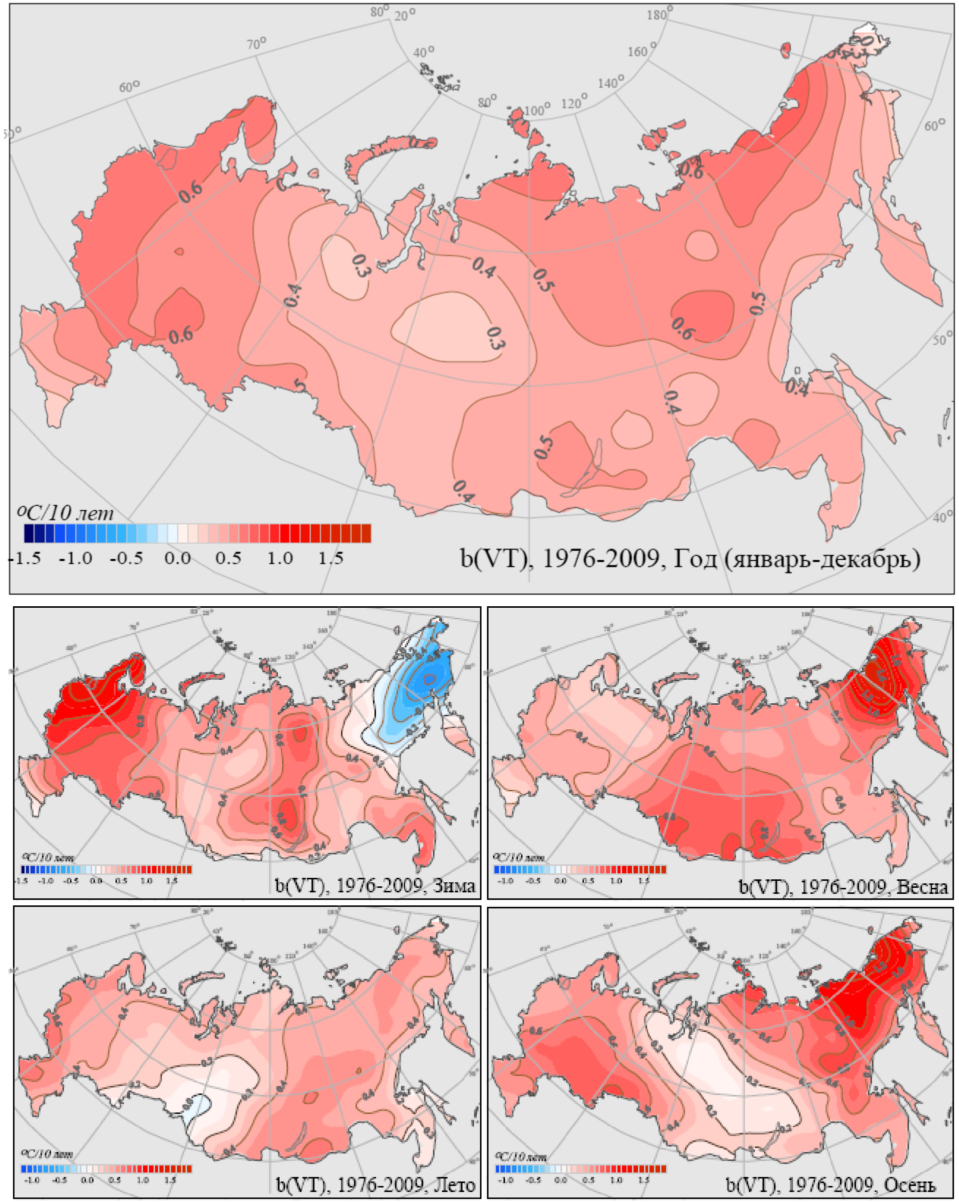

Surface air temperature trends (K/10 years) for 1976-2009

by data from Rosgidromet

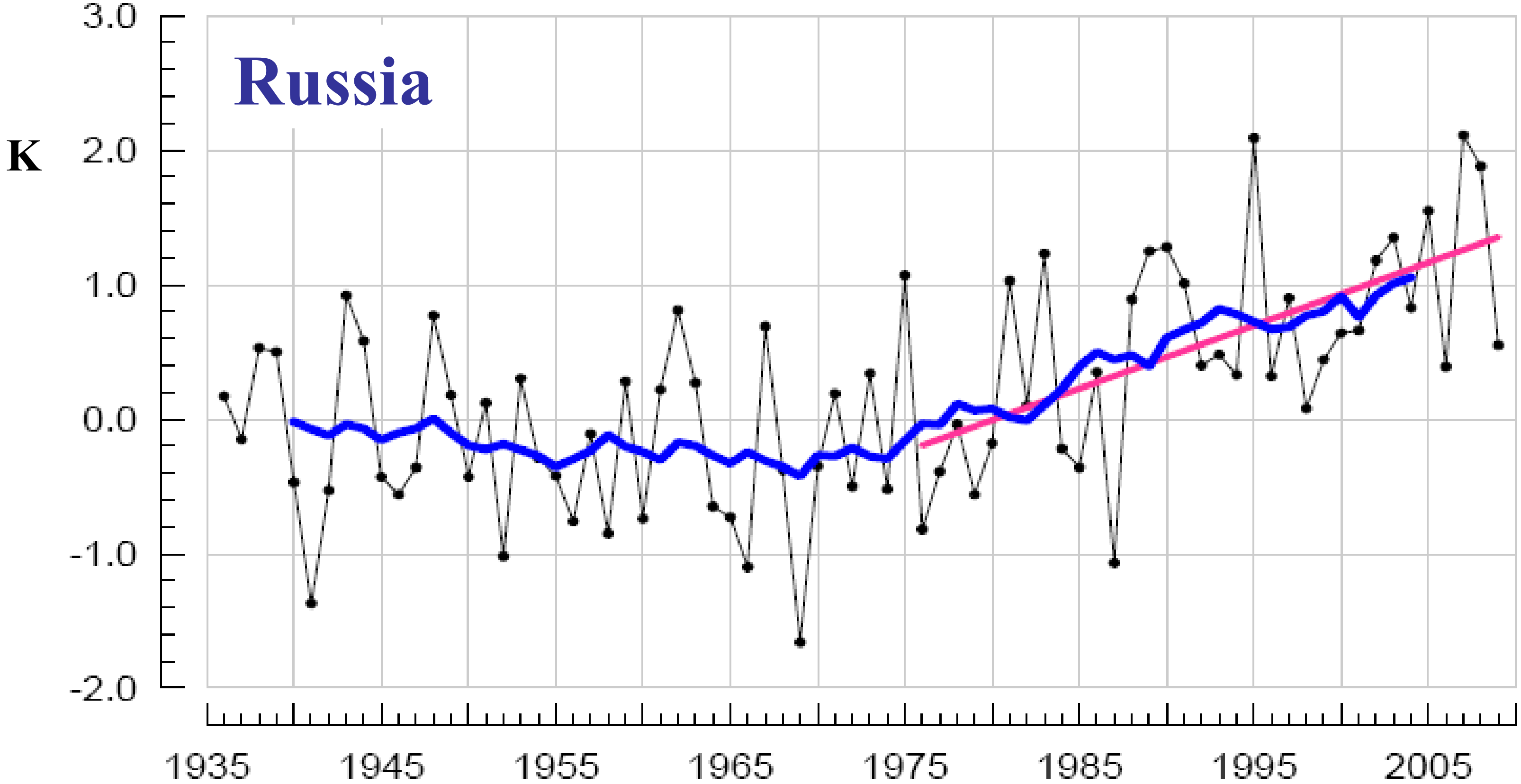

Interannual variations of surface air temperature (relative 1961-1990).

Red line – SAT trend (1976-2009). Blue curve – with 11-year averaging.

1976-2009: 0.47 K/10 years (contribution to the variance - 34%)
1976-2008: 0.52 K/10 years (35%)
1976-2007: 0.48 K/10 years (34%)

by data from Rosgidromet

Surface air temperature trends (b, K/10 years) in Russian regions during 1976-2009

D – linear trend contribution (%) to the variance

Region	Annual		Winter		Spring		Summer		Autumn	
	b	*D%*	*b*	*D%*	*b*	*D%*	*b*	*D%*	*b*	*D%*
Russia	0.47	35	0.44	7	0.58	27	0.38	48	0.51	20
European part of Russia	0.56	34	0.83	14	0.37	11	0.43	22	0.60	22
Western Siberia	0.36	16	0.40	3	0.62	16	0.16	4	0.36	5
Middle Siberia	0.46	21	0.50	4	0.60	17	0.41	27	0.36	4
Baikal Lake Region, Transbaikalia	0.46	29	0.44	5	0.71	26	0.54	40	0.24	4
Eastern Siberia	0.51	35	-0.14	2	0.82	30	0.46	38	0.86	38
Primorye & Priamurye	0.42	38	0.54	12	0.41	14	0.25	17	0.49	26

by Rosgidromet data

100-year moving trends of global and hemispheric surface temperature

CRU

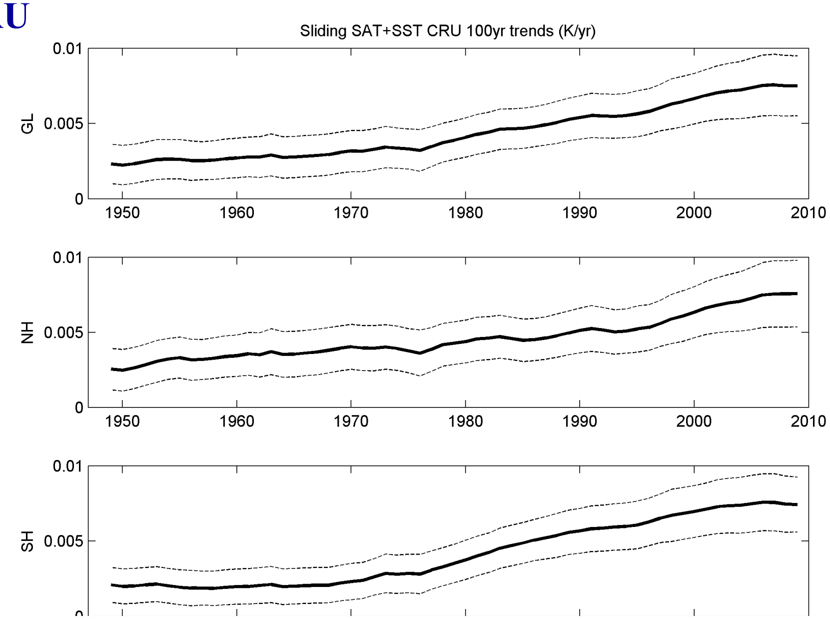

GISS

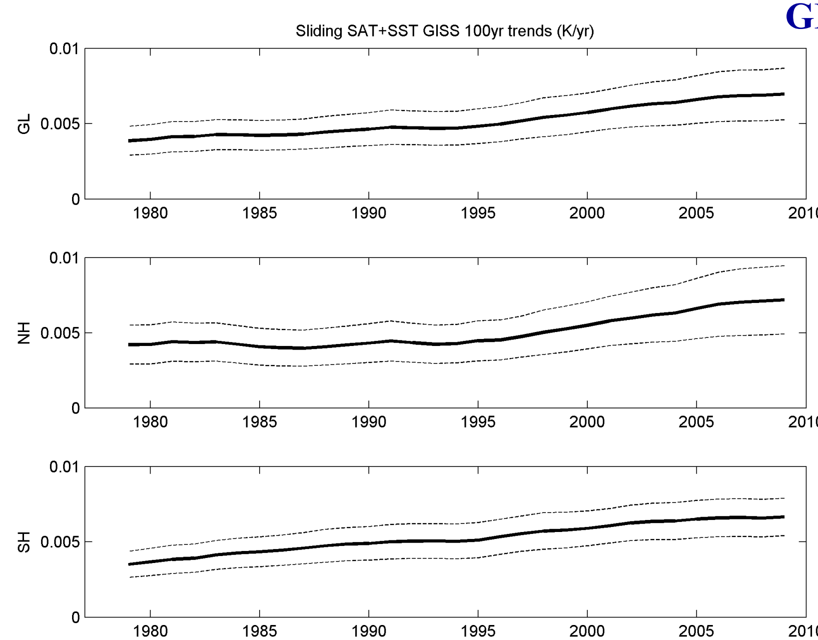

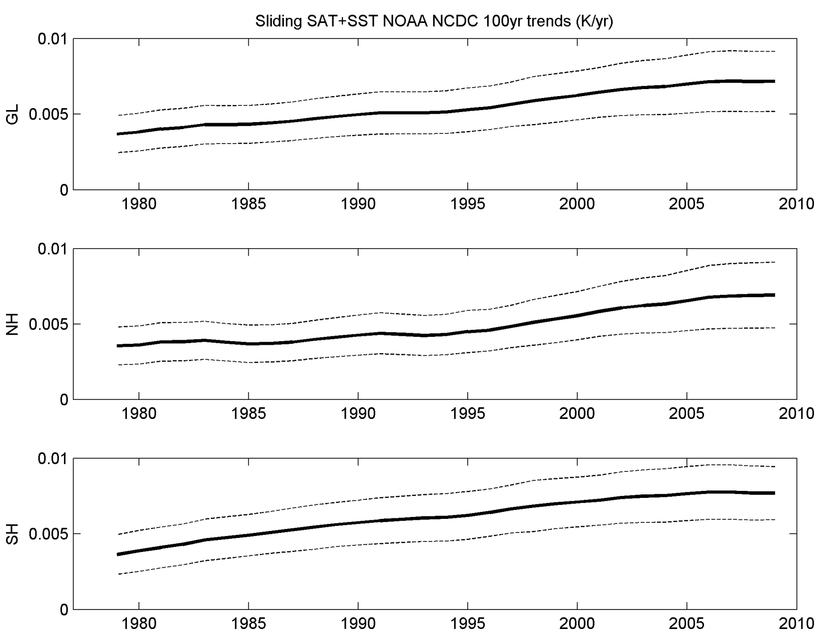

NCDC

by CRU, GISS and NCDC data

Mokhov and Karpenko

Cross-wavelet analysis (local coherency and phase lag) of variations for global surface temperature (by CRU data) and solar irradiance (by different data: a - Lean, b - Hoyt)

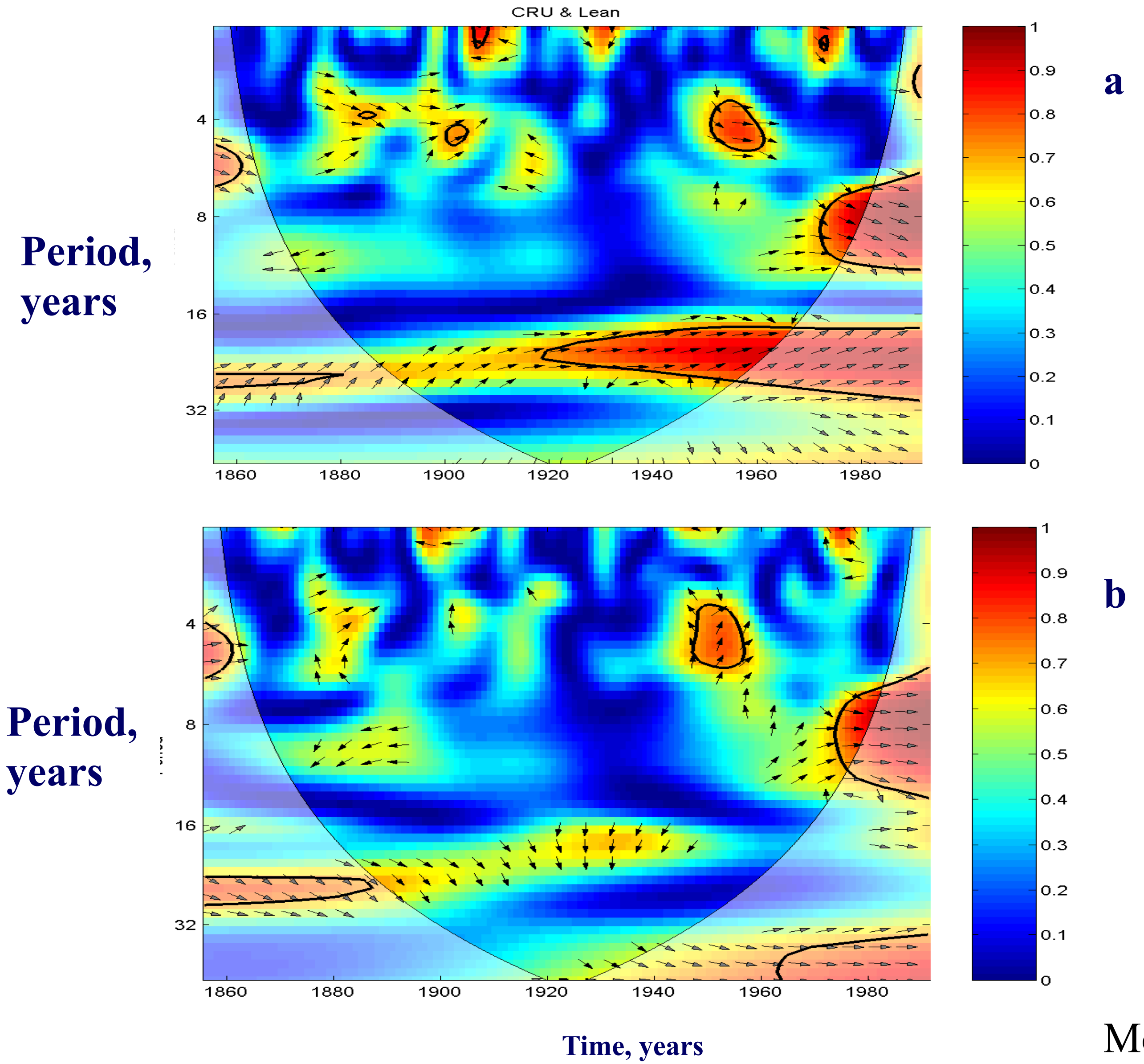

Mokhov and Karpenko

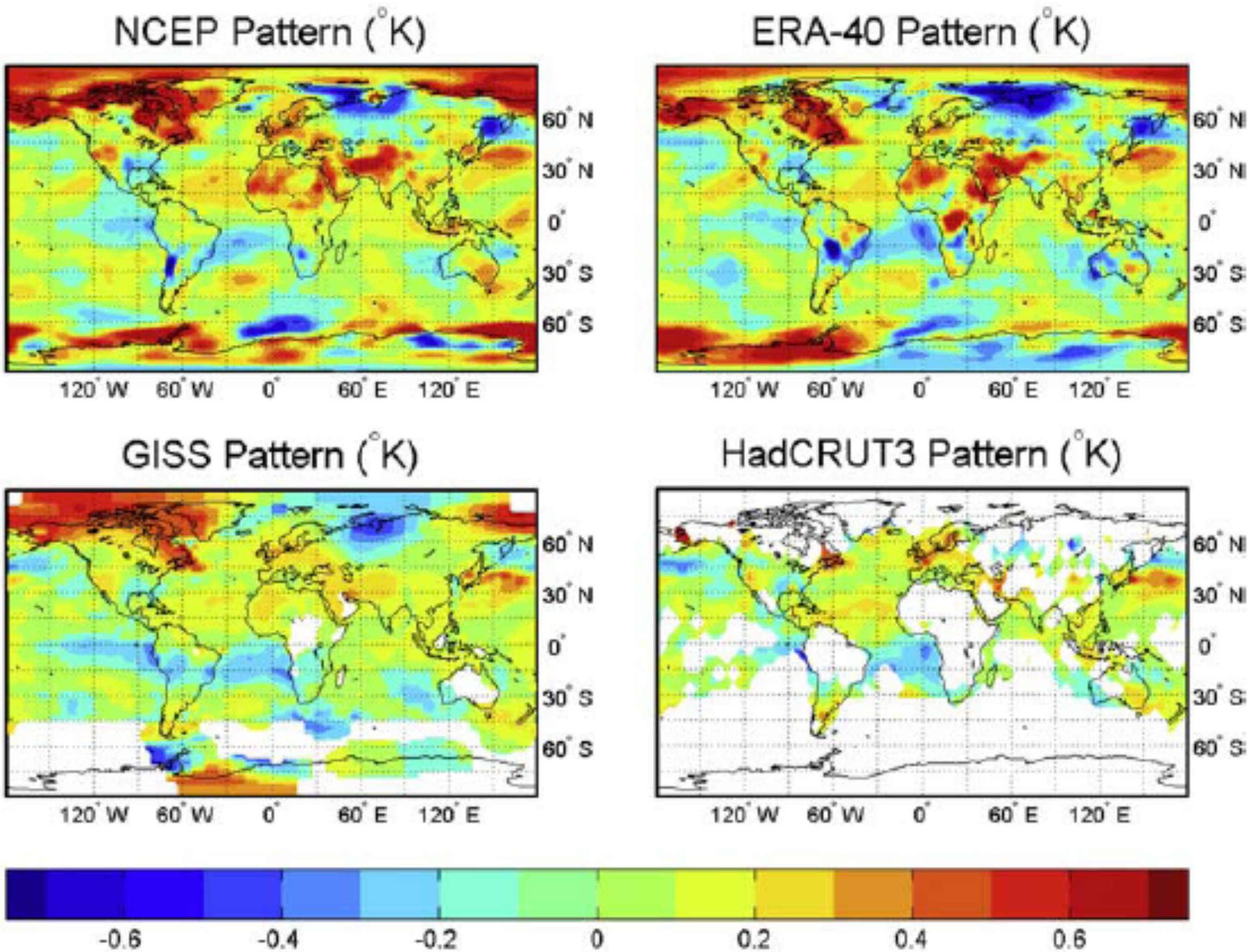

Composite mean difference between solar max years and solar min years in surface temperature in K; missing data areas are left blank. Annual average is the average of seasons, provided that at least three seasons are available and the missing season is not winter or summer. Seasonal average is the average of three months in the season, provided that at least two months are available.

Tung et al.

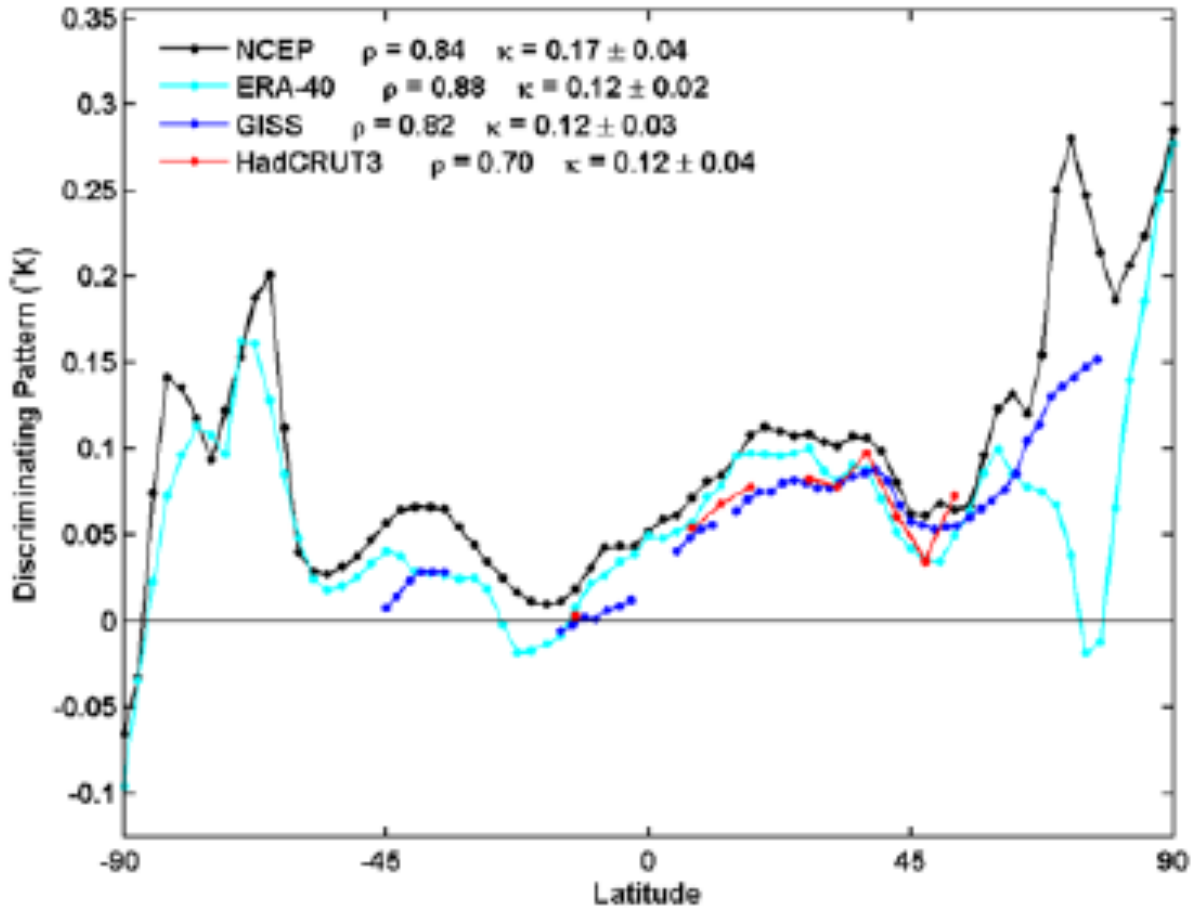

Zonal mean spatial pattern that best distinguishes solar max years from the solar min years

Tung et al.

Cross-wavelet analysis (local coherency and phase lag) of variations for global surface temperature (by CRU data) and CO2 concentration (by data for Mauna Loa)

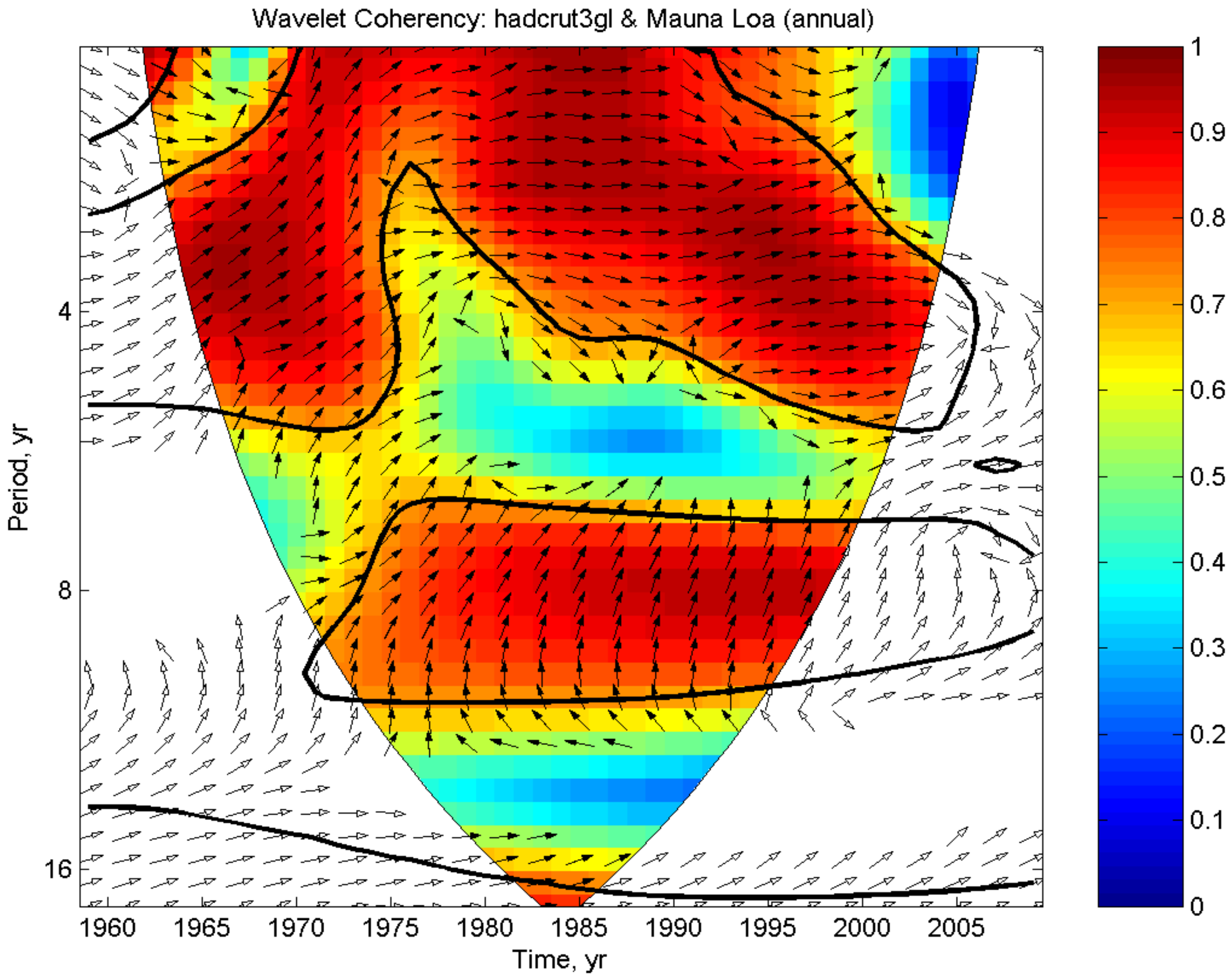

Cross-wavelet analysis (local coherency and phase lag) of variations for global surface temperature (by CRU data) and CO2 concentration (by data for Mauna Loa)

Wavelet analysis

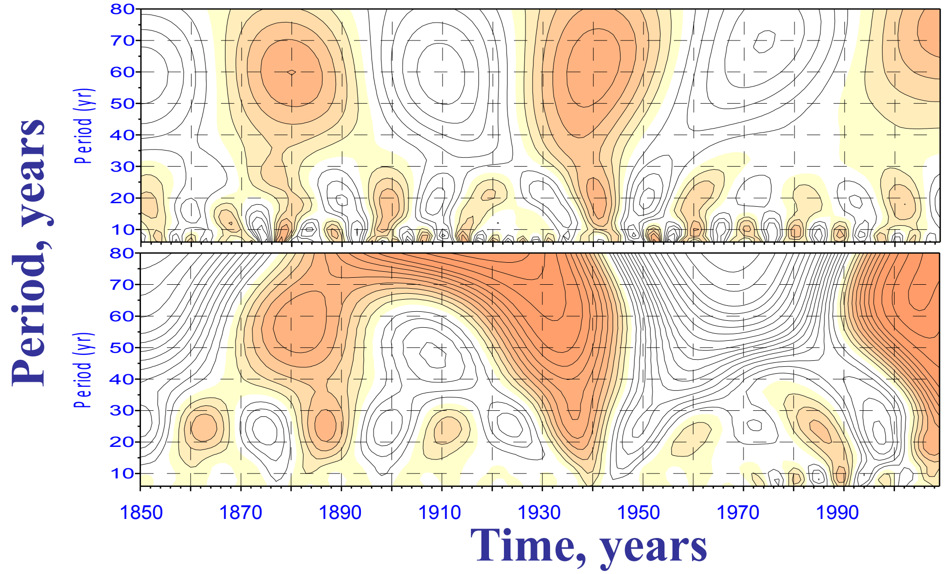

Temperature

CO_2

Cross-wavelet analysis

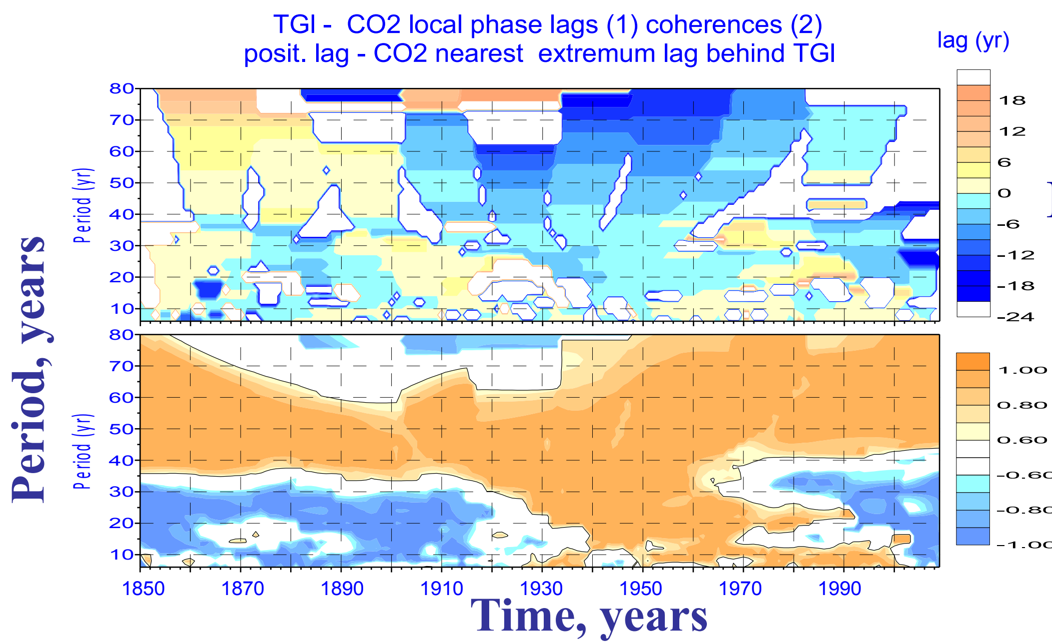

Phase lag

Coherency

Granger causality

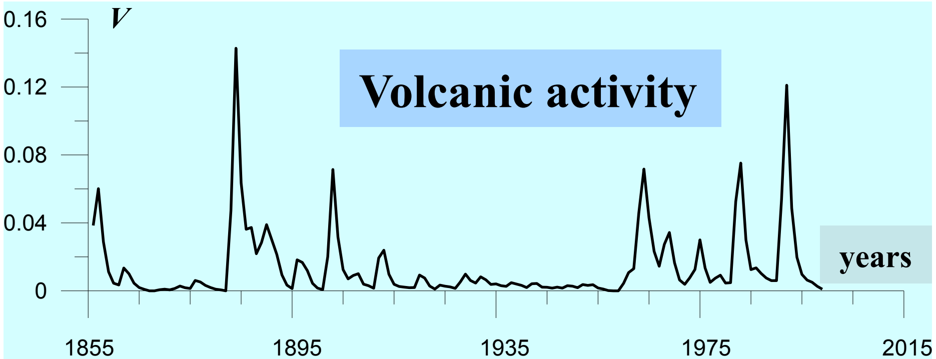

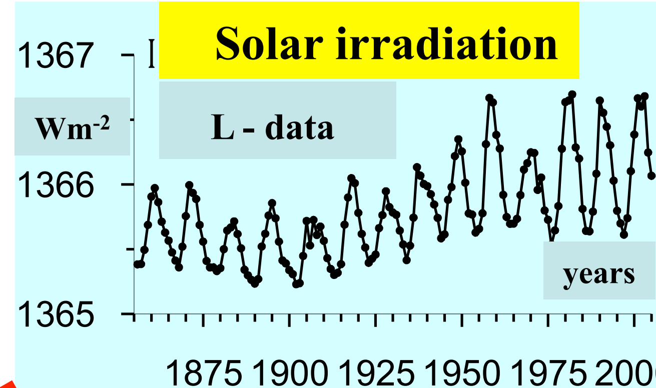

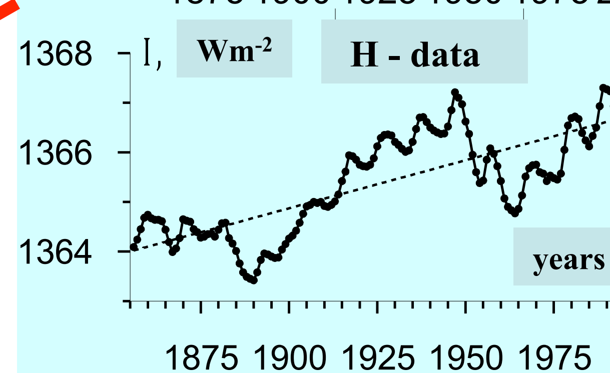

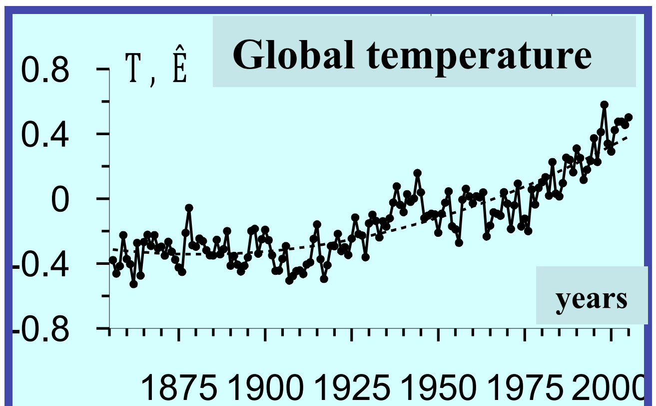

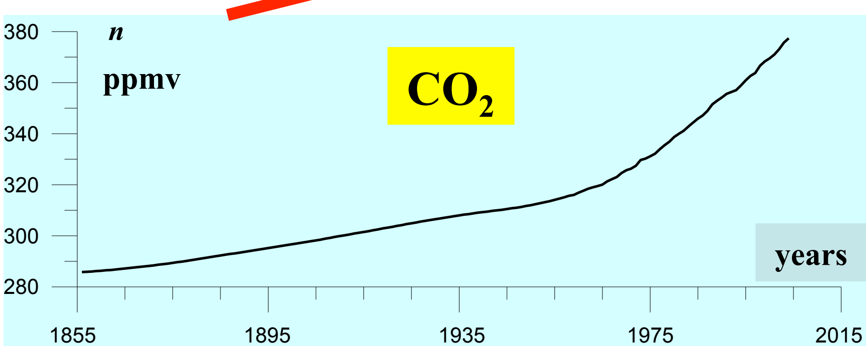

Analysis of individual and joint influence

Mokhov & Smirnov

Empirical predictive models and Granger causality (prediction improvement)

Two series: *x* and *y*

$x_t, y_t, t = 1, \ldots, N$

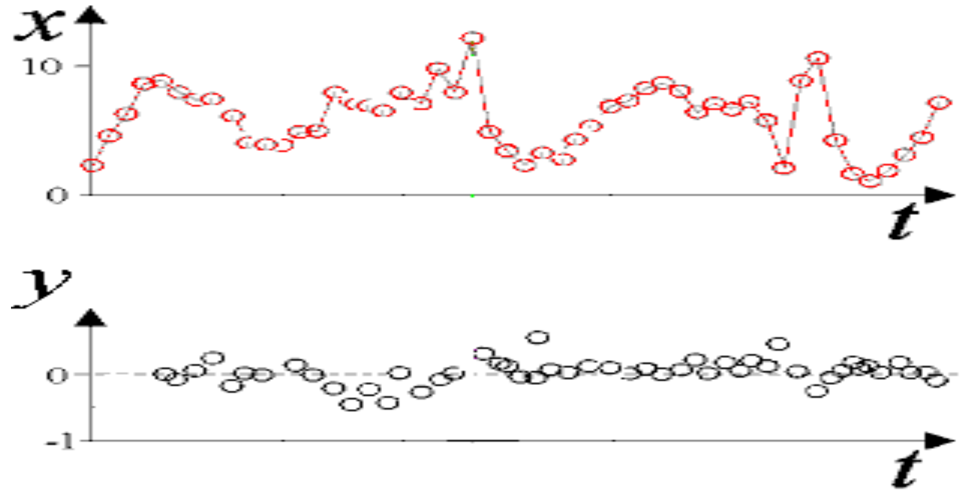

Individual model

$$x_t = f(x_{t-1}, x_{t-2}, \ldots, x_{t-d_1}, \mathbf{a})$$

Its prediction error

$$\sigma_x^2(d_1) = \left\langle \left[x_t - f(x_{t-1}, x_{t-2}, \ldots, x_{t-d_1}, \hat{\mathbf{a}}) \right]^2 \right\rangle_t$$

Joint model

$$x_t = F(x_{t-1}, x_{t-2}, \ldots, x_{t-d_1}, y_{t-1}, y_{t-2}, \ldots, y_{t-d_2}, \mathbf{a})$$

Its prediction error

$$\sigma_{x|y}^2(d_1, d_2) = \left\langle \left[x_t - F(x_{t-1}, \ldots, x_{t-d_1}, y_{t-1}, \ldots, y_{t-d_2}, \hat{\mathbf{a}}) \right]^2 \right\rangle_t$$

Prediction improvement of *x* (when *y* is incorporated into a model) is a sign of influence *y*→*x*

$$PI_{y \to x}(d_1, d_2) = \sigma_x^2(d_1) - \sigma_{x|y}^2(d_1, d_2)$$

Bivariate models (T:I, T:V, T:n)

$$T(t) = a_1 T(t-1) + a_4 T(t-4) + b_I I(t-1) + \xi(t)$$

$$T(t) = a_1 T(t-1) + a_4 T(t-4) + b_V V(t) + \xi(t)$$

$$T(t) = a_1 T(t-1) + a_4 T(t-4) + b_{1,n} n(t-1) + b_{2,n} n(t-2) + \xi(t)$$

Joint model (T:I,V,n)

$$T(t) = a_1 T(t-1) + a_4 T(t-4) + b_I I(t-1) + b_V V(t) + b_{1,n} n(t-1) + b_{2,n} n(t-2) + \xi(t)$$

According to the empirical models, the rise in CO_2 concentration determines at least 75% of the GST trend in 1985−2005, while the other two factors (forcings) are not the causes of the global warming. In particular, if the CO2 concentration remained at the level of 1856 year, the GST would not rise during the last century. In contrast, variations in solar and volcanic activity would not lead to significant changes in the GST trend. All the influences are detected if the data at least for the interval [1856−1940] are used for the model fitting.

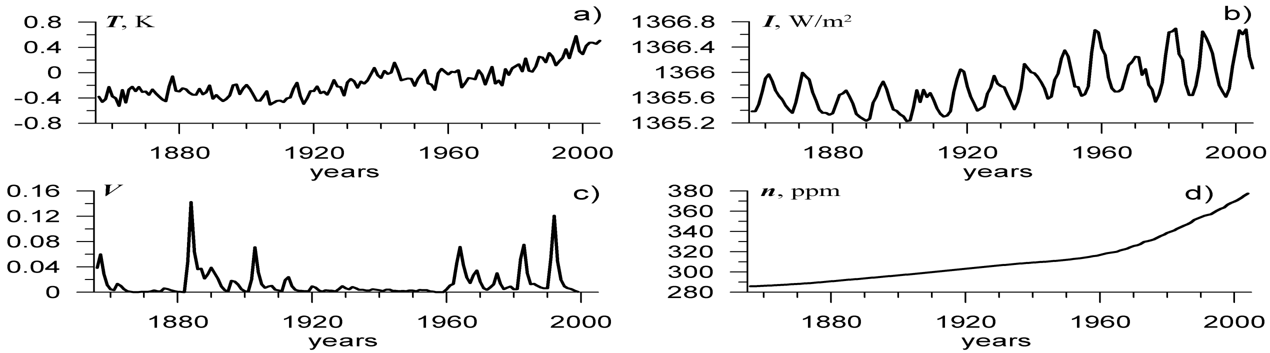

The data used: a) GST - global surface temperature (anomalies relative 1961−1990); b) solar constant (W/m^2); c) volcanic activity (optical depth of volcanic aerosol); d) CO_2 atmospheric content in ppm (parts per million).

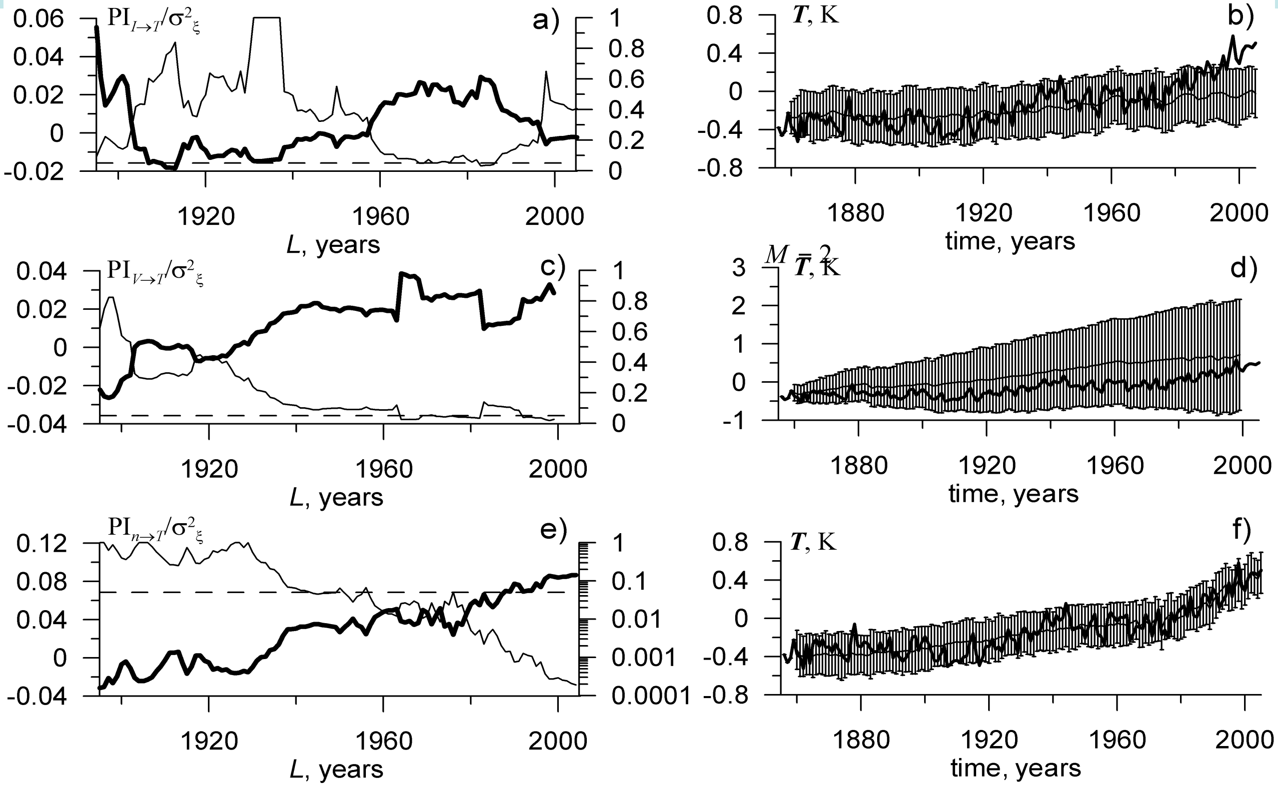

Solar variations

Volcanic activity

CO_2 content variations

(Mokhov & Smirnov, 2009)

Bivariate models of GST fitted to different time intervals [1856−L]: a) models with solar activity; b) models with volcanic activity; c) models with CO_2 atmospheric content. The normalized values of prediction improvement (the thick lines) are indicated on the left y-axes (dimensionless), significance levels (the thin lines) on the right y-axes (dimensionless). The dashed lines show the level of p = 0.05.

Cause-and-effect relations of climatic processes (ENSO, NAO/AO, EAM, Monsoon, AMO, …)

Long-term causality (which extends the concept of Granger causality) was also applied to find out how strongly the global surface temperature (GST) is affected by variations in carbon dioxide atmospheric content, solar activity, and volcanic activity during the last 150 years.

It was noted mutual influence for GST and CO_2 Despite influences of all the three factors are detected with the Granger causality, the long-term causality shows that the rise in GST during the last decades can be explained only if the anthropogenic factor (CO_2) is taken into account.

It was analyzed also influence on GST of different indices characterizing multidecadal climate cycles, including Earth rotation and Atlantic Multidecadal Oscillation (thermohaline circulation). In particular, Earth rotation influence was noted only for GST variations with relatively short periods of comparison to the CO_2 influence on long-term trends.

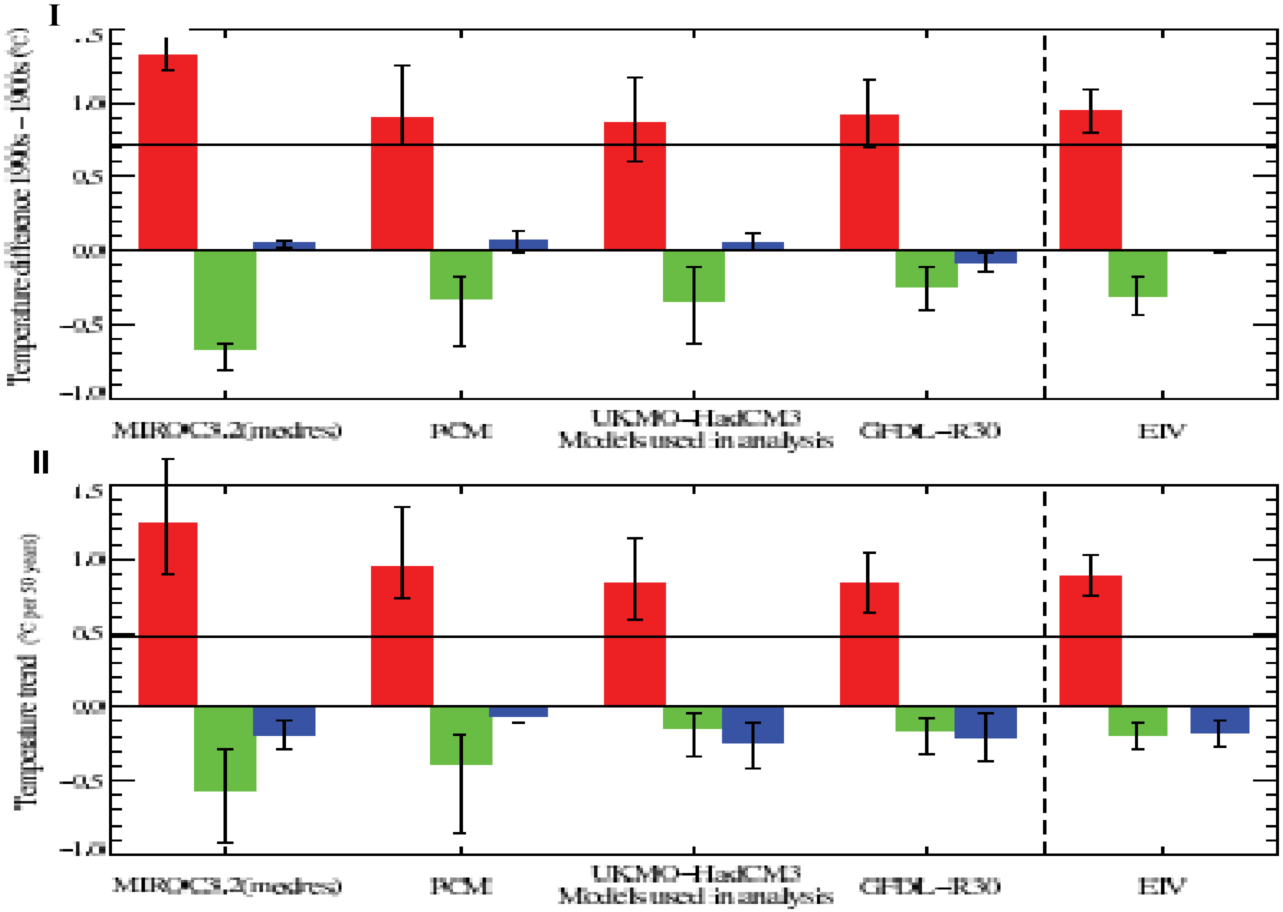

Estimated contribution from greenhouse gases (red), other anthropogenic (green) and natural (blue) components to observed global surface temperature changes. (I) the estimated contribution of forced changes to temperature changes over the 20th century, expressed as the difference between 1990 to 1999 mean temperature and 1900 to 1909 mean temperature (K) and (c) estimated contribution to temperature trends over 1950 to 1999 (K per 50 years). The horizontal black lines in (I) and (II) show the observed temperature changes from CRU data. The results from ensembles of simulations containing each set of forcings separately are shown for four models, MIROC3.2, PCM, UKMO-HadCM3 and GFDL-R30. EIV - combined response from three models (PCM, UKMO-HadCM3 and GFDL-R30) for each of the three forcings separately, thus incorporating inter-model uncertainty.

IPCC-2007

Assessment of surface temperature trends (K/decade) due to different causes for various 50-years periods

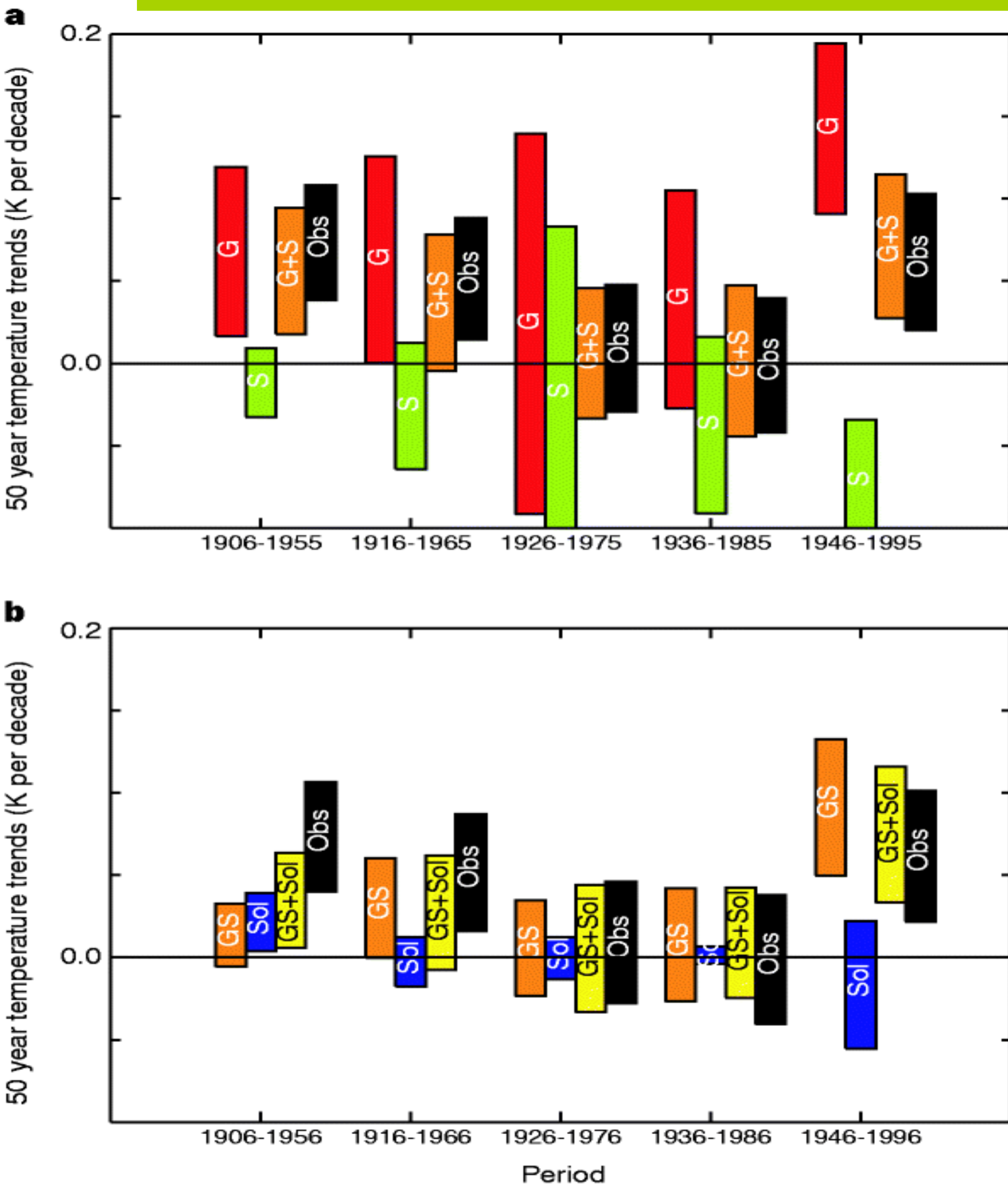

Black – observations,
Blue – solar irradiation (Sol),
Red – greenhouse gases (G),
Green – anthropogenic aerosol (S),
Orange - (G+S),
Yellow - (G+S+Sol).

	F-test*				
	1906–56	1916–66	1926–76	1936–86	1946–96
Int. var.†	**0.01**	**0.04**	0.69	0.76	**0.01**
G	0.18^{G}	0.11	0.75	0.80	0.10^{G}
GS	0.06^{GS}	0.23	0.76	0.85	0.30^{GS}
Sol†	0.11^{Sol}	0.06	0.75	0.87	**0.03**
Vol†	**0.03**	0.08	0.74	0.80	**0.04**†
G&S	0.21^{G}	0.17^{G}	0.68	0.83	$0.31^{G,S}$
G&Sol	0.23^{G}	$0.17^{G,Sol}$	0.68	0.81	0.07^{G}
G&Vol	0.24^{G}	0.09	0.67	0.73	0.08^{G}
GS&Sol	0.13^{Sol}	0.19^{GS}	0.68	0.82	0.25^{GS}
GS&Vol	0.05^{GS}	0.22^{GS}	0.68	0.80	0.25^{GS}
Sol&Vol†	0.08^{Sol}	0.09‡	0.67	0.82	**0.04**‡

* These columns show the probability (*P*) that the best-fit signal combination is consistent with observations using an *F*-test with 21 degrees of freedom. Values in bold are inconsistent with the observations. When a signal is detected, its name is shown as a superscript next to the *P*-value. Actual *P*-values are shown, although 0.03 is the lowest value that can be robustly estimated given the available length of Control.
† Signal combination is an inadequate explanation of twentieth-century temperature change as the *F*-test fails at least once.
‡ Volcanic amplitude in this signal-combination is significantly negative and thus unphysical. No other signal ever has a significant negative amplitude.

Tett et al.

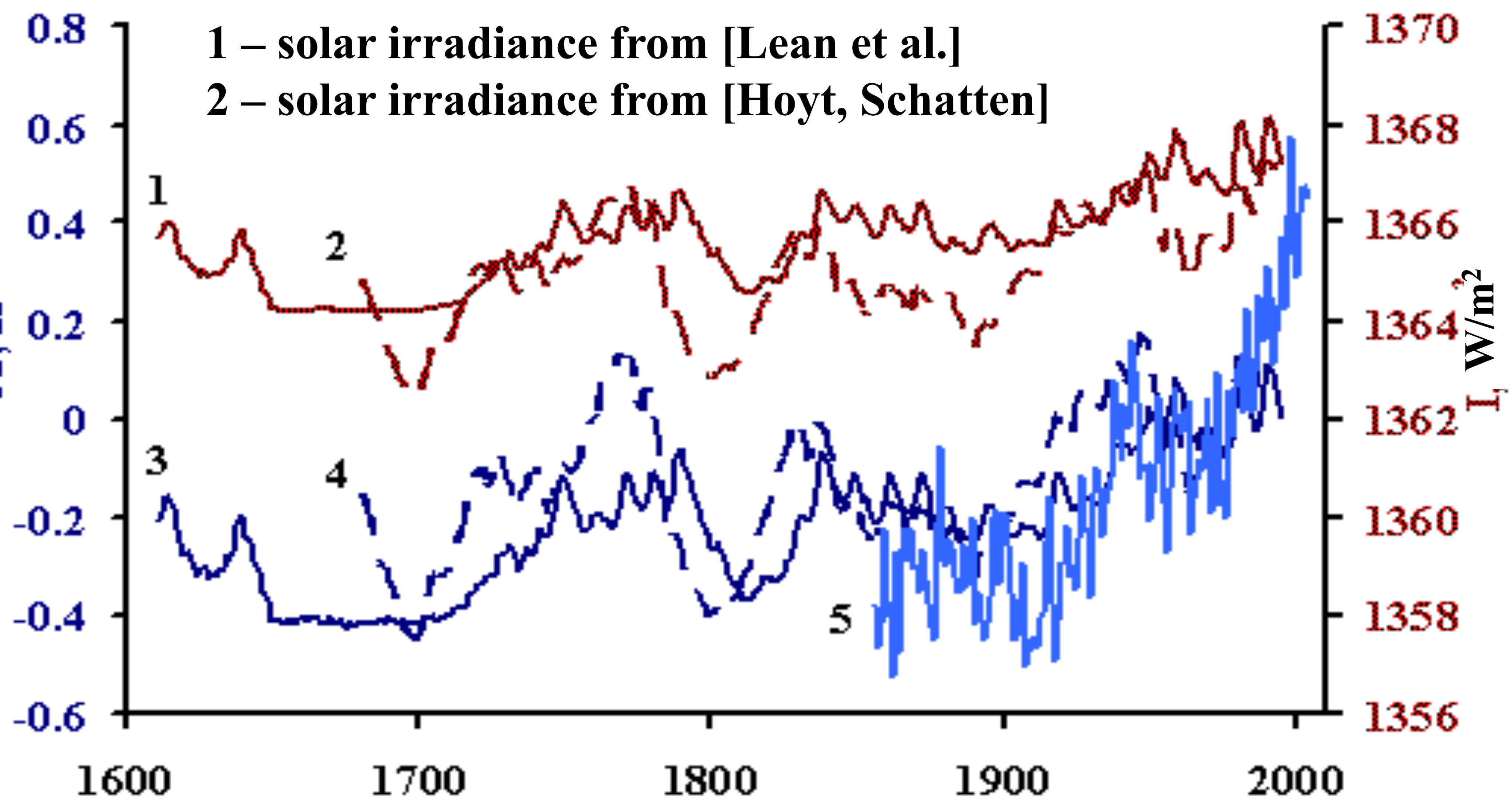

Variations of solar irradiance *I* (W/m^2) (1, 2) and associated global surface temperature variations δT (K) (3,4) from simulations with the IAP RAS climate model in comparison with temperature variations from observations (CRU) (5).

Mokhov, Bezverkhny, Eliseev & Karpenko

Surface temperature differences between years with maximum and minimum solar irradiance during last 5 decades from simulations with IAP RAS climate model

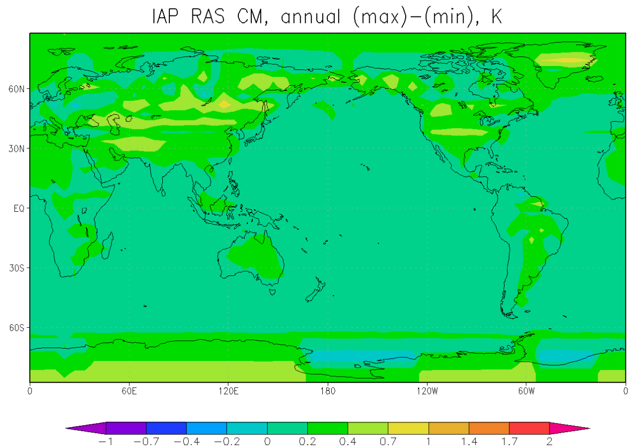

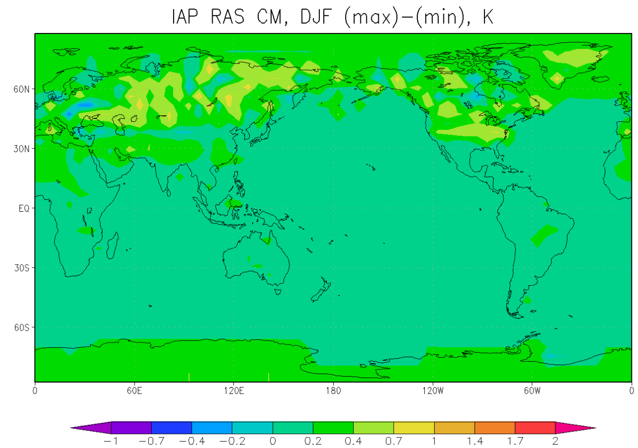

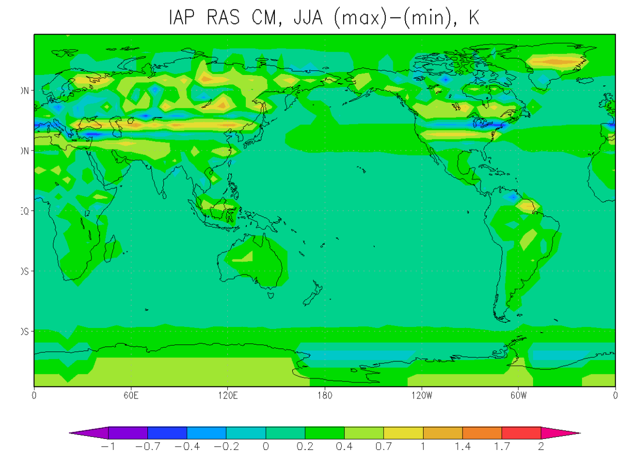

annual

December-January-February

June-July-August

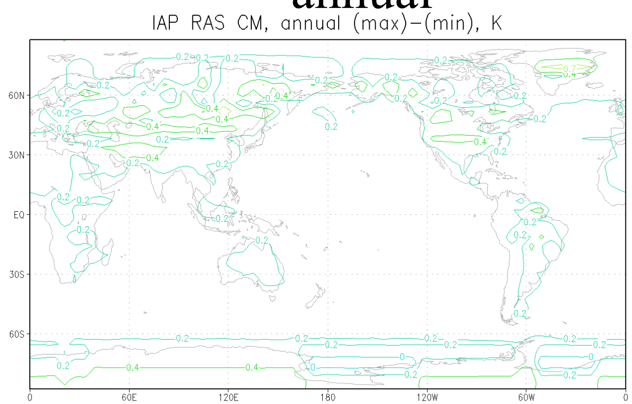

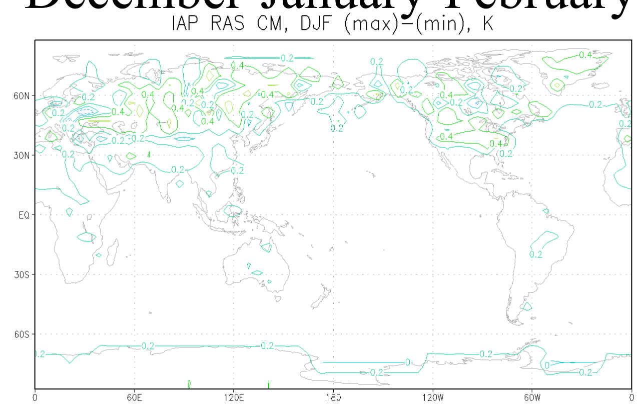

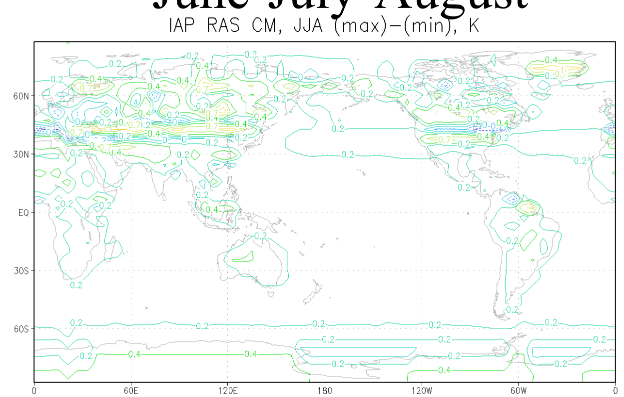

Mokhov, Eliseev & Karpenko

Temperature trends during the last 3 decades of the 20th century from simulations with HadCM3 and IAP RAS climate model under different scenarios (forcings)

Trend T_a, K/10 years 1970-1999		Combined	Anthropogenic	Natural
Siberia (Irkutsk)	HadCM3	0.34 (±0.13)	0.32 (±0.09)	0 (±0.08)
	IAP RAS CM	0.16 (±0.13)	0.29 (±0.12)	0.08 (±0.13)
Alaska (Barrow)	HadCM3	0.51 (±0.18)	0.54 (±0.18)	-0.08 (±0.02)
	IAP RAS CM	0.19 (±0.07)	0.18 (±0.06)	-0.07 (±0.05)
Antarctic Peninsula (Bellingshausen)	HadCM3	0.43 (±0.14)	0.34 (±0.13)	0.06 (±0.14)
	IAP RAS CM	0.12 (±0.07)	0.12 (±0.12)	0 (±0.03)

Mokhov, Karpenko & Stott

Ensemble simulations with the IAP RAS climate model of intermediate complexity for different natural and anthropogenic scenarios

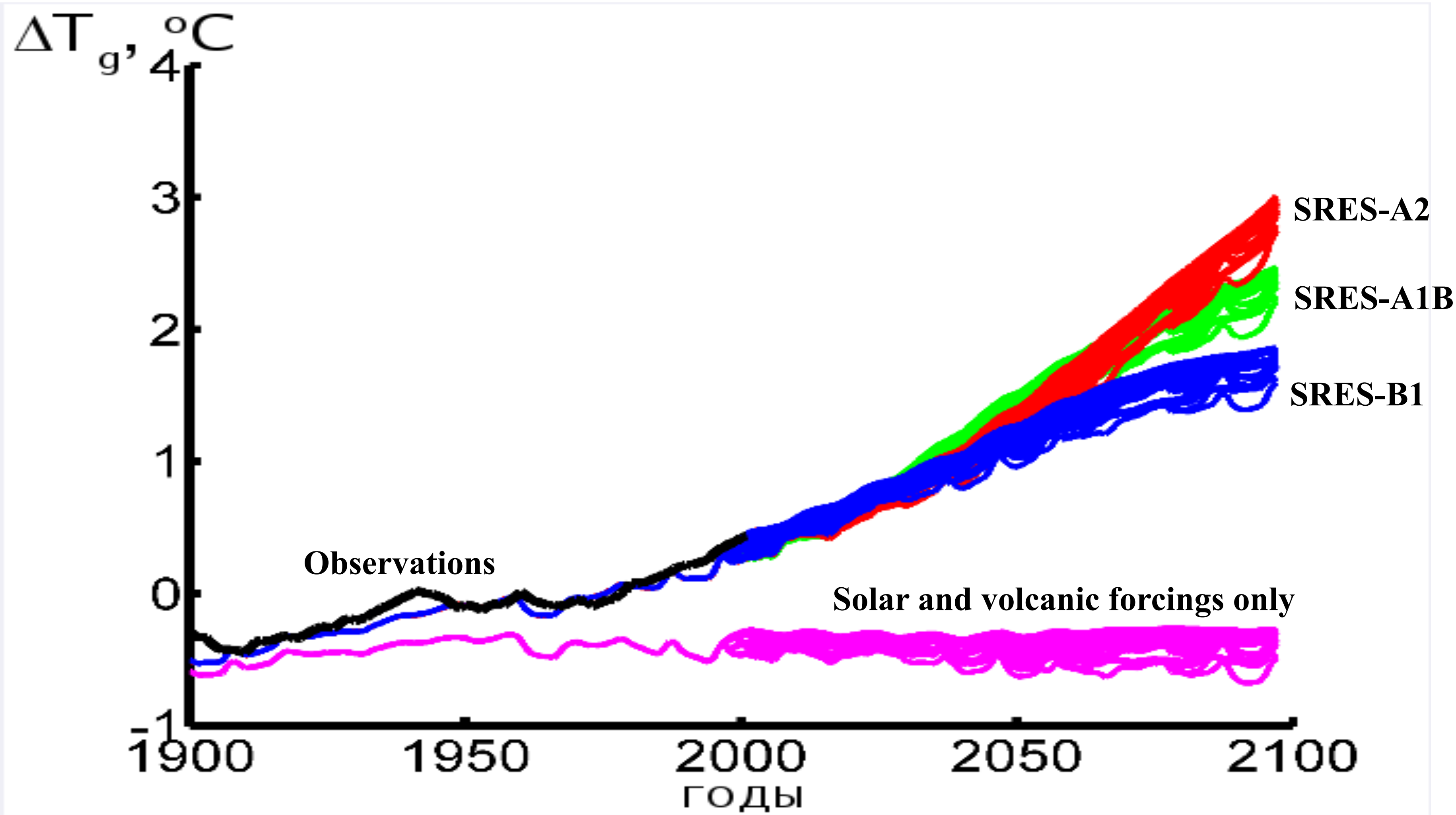

Mokhov I.I. et al.

Temperature trends during the last 3 decades of the 20th century from simulations (HadCM3) with different initial conditions

Trend T_α, K/10 years 1970-1999 HadCM3		Combined	Anthropogenic	Natural
Antarctic Peninsula	1	0.72	0.37	-0.23
	2	0.48	0.26	0.34
	3	0.23	0.33	-0.13
	4	0.30	0.40	0.27
Siberia	1	0.48	0.23	0.12
	2	0.35	0.17	0.05
	3	0.18	0.48	-0.09
	4	0.36	0.38	-0.08
Alaska	1	0.64	0.30	0.16
	2	0.39	0.27	-0.17
	3	0.11	0.83	-0.14
	4	-0.15	0.75	-0.17

Thank you

for your attention